Supporting Information

Selective recognition of small hydrogen bond acceptors by a calix[6]arene-based molecular container

Roy Lavendomme,[a,b] Florent Desroches,[b] Steven Moerkerke,[a] Filip Topić,[c] Johan Wouters,[d] Kari Rissanen,[c] Michel Luhmer,[b] Ivan Jabin*[a]*

[a] Laboratoire de Chimie Organique, Université libre de Bruxelles (ULB), Avenue F.D. Roosevelt 50, CP160/06, B-1050 Brussels, Belgium.
[b] Laboratoire de Résonance Magnétique Nucléaire Haute Résolution, Université libre de Bruxelles (ULB), Avenue F.D. Roosevelt 50, CP160/08, B-1050 Brussels, Belgium.
[c] University of Jyväskylä, Department of Chemistry, Nanoscience Center, P.O. Box 35, FI-40014, Finland.
[d] Département de Chimie, Université de Namur (UNamur), Rue de Bruxelles 61, B5-5000 Namur, Belgium.

* Roy Lavendomme, e-mail: rlavendomme@gmail.com
* Ivan Jabin, e-mail: ijabin@ulb.ac.be

Table of Contents

Experimental Section

NMR spectra were recorded either at 7.0, 9.4 or 14.1 Tesla. Solvent signals were used as internal standards for ^{1}H (7.16 ppm for C_6D_5H, 7.26 ppm for $CHCl_3$, 5.32 ppm for $CHDCl_2$, 6.00 ppm for $CDCl_2CHCl_2$) and ^{13}C (128.06 ppm for C_6D_6, 77.16 ppm for $CDCl_3$) chemical shift referencing. Edited HSQC refers to multiplicity-edited sequence showing CH_2 correlation spots in negative phase (blue) and CH/CH_3 correlation spots in positive phase (red). Bac stands for *tert*-butylaminocarbonyl. $BARF^-$ stands for tetrakis(3,5-bis(trifluoromethyl)phenyl)borate.

Guest screening for host 2

We screened the following potential guests in presence of host **2** in $CDCl_3$ by ^1H NMR spectroscopy: K_2CO_3, Cs_2CO_3, $TBA^+NO_3^-$, $NMe_4^+Cl^-$, $NMe_4^+BARF^-$, octane-1,8-diol, acetic acid, sulfolane, acetone, acetamide, succinimide, 2-imidazolidinone (Imi), DMSO, imidazole, pyrazole, thiazole, ethylamine, isopropylamine, and pyrrolidine. No significant variation in the ^1H NMR spectrum of **2** occurred upon addition of the salts, sulfolane and acetone in excess. Significant changes were observed upon addition of the other guests (Figures S1-S4). These changes were attributed to the formation of inclusion complexes due to the diminishing intensities of self-included *t*Bu signals initially observed for the free host **2**.

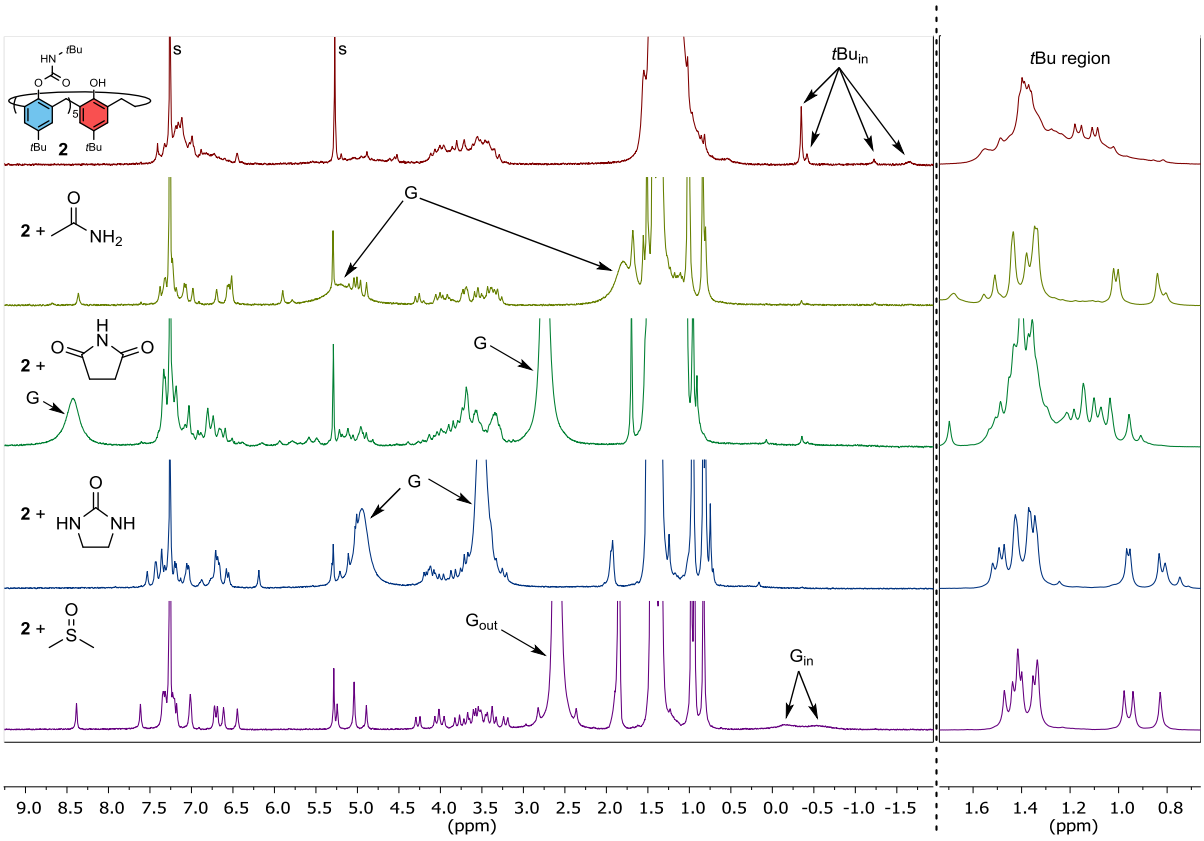

Figure S1. ^1H NMR spectra (300 MHz, $CDCl_3$, 298 K) of host **2** and its complexes with carbonyl or sulfoxide bearing guests (up to 25 equiv.): acetamide, succinimide, 2-imidazolidinone (Imi), and DMSO. s: residual solvents. G: guest.

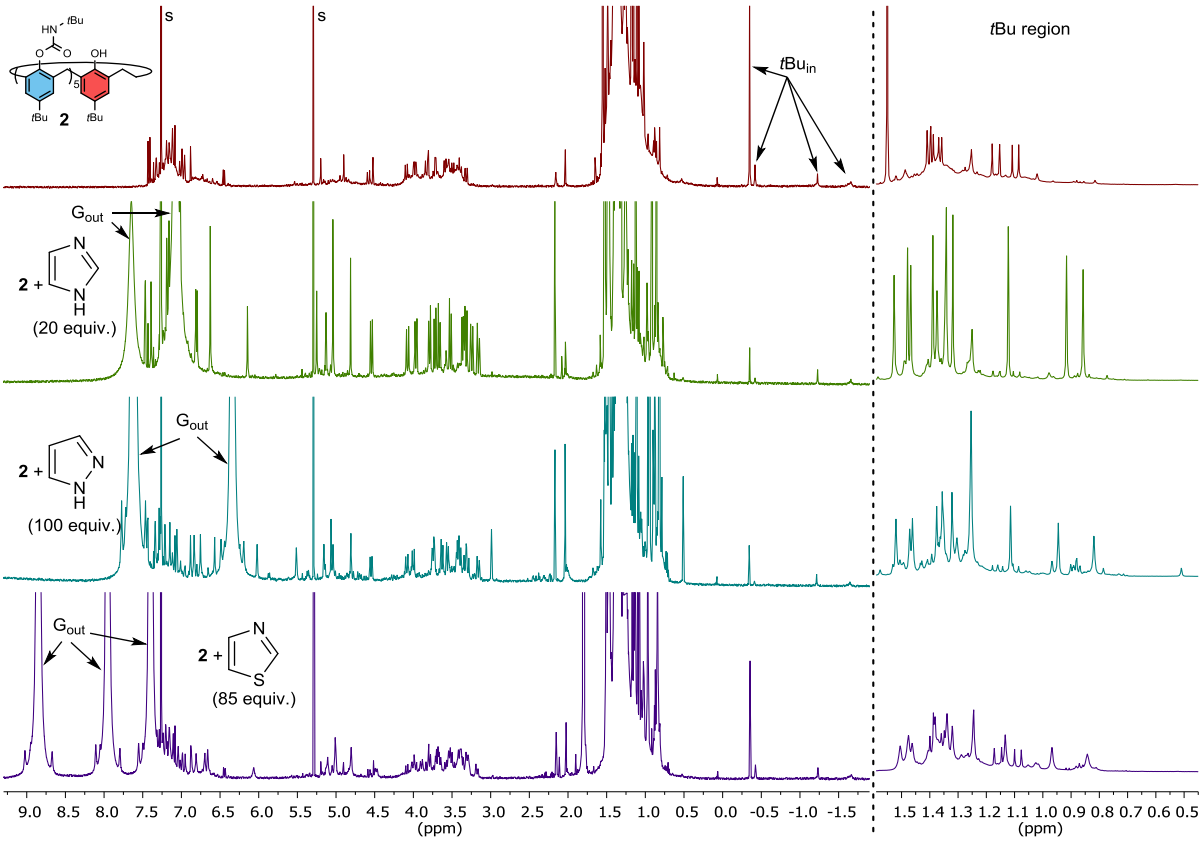

Figure S2. ^{1}H NMR spectra (600 MHz, $CDCl_3$, 298 K) of host **2** (2 mM) and its complexes with azole guests: imidazole, pyrazole, and thiazole. s: residual solvents. G: guest.

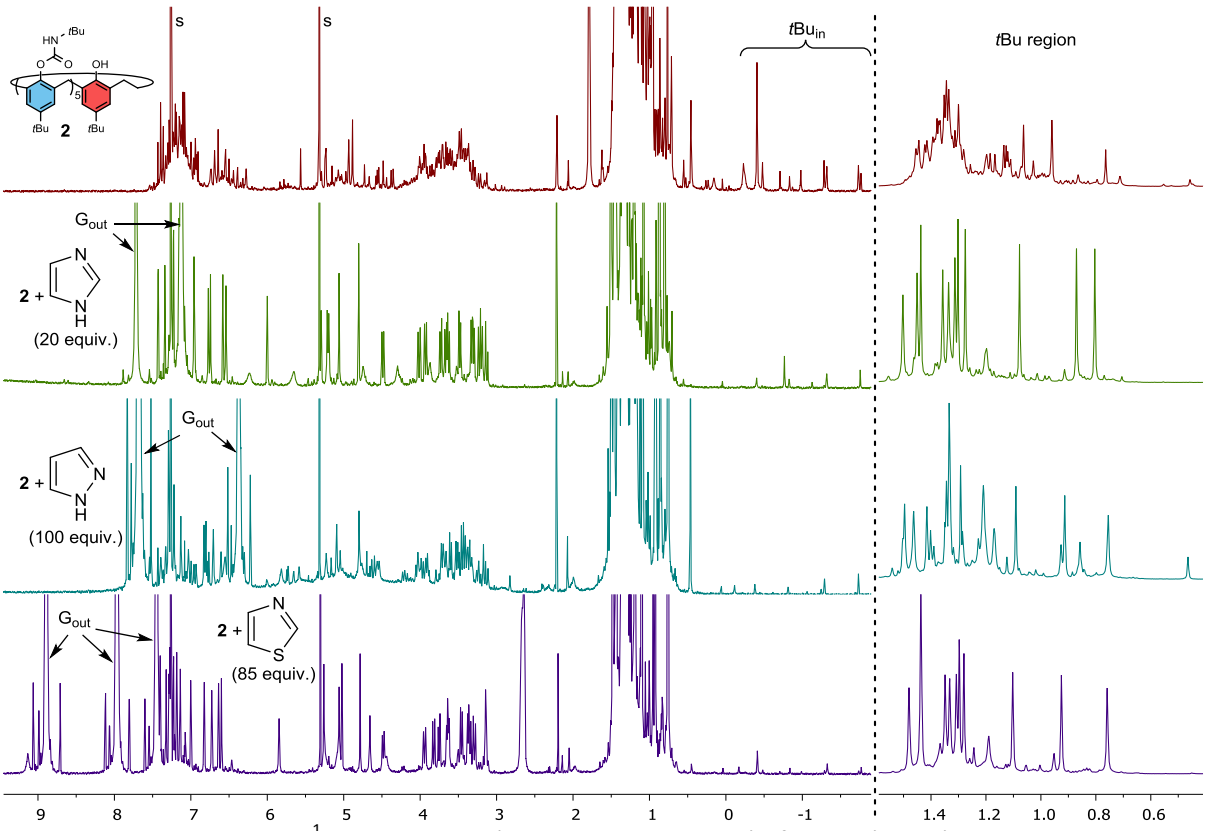

Figure S3. Low temperature ^{1}H NMR spectra (600 MHz, $CDCl_3$, 223 K) of host **2** (2 mM) and its complexes with azole guests: imidazole, pyrazole, and thiazole. s: residual solvents. G: guest.

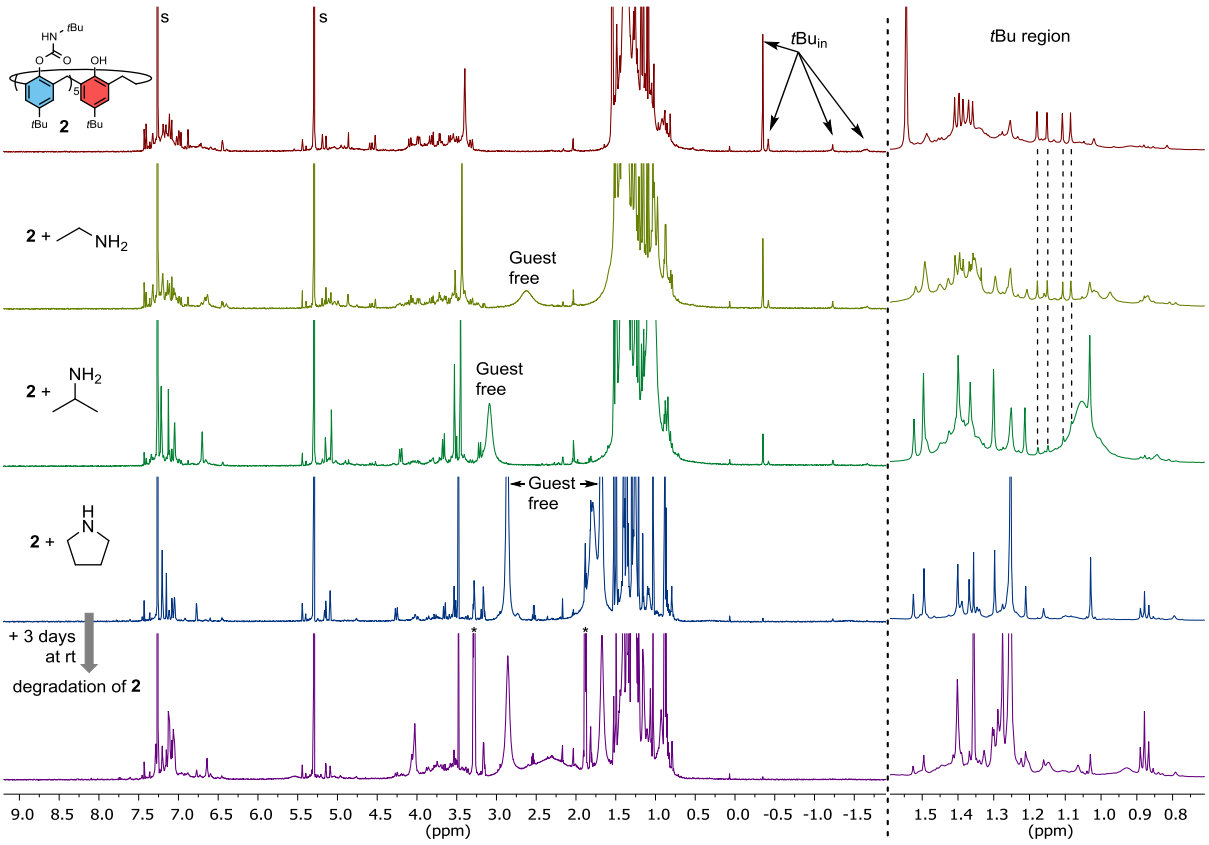

Figure S4. ^{1}H NMR spectra (600 MHz, $CDCl_3$, 298 K) of host **2** (2 mM) and its complexes with amine guests (20 mM): ethylamine, isopropylamine, and pyrrolidine. The intensity of free host **2** signals in presence of the different guests (see dashed lines in the *t*Bu region) indicates that the binding strength follows the order pyrrolidine > isopropylamine > ethylamine. The host **2** was observed to degrade over time in presence of amines as shown in the bottom spectrum. *: likely pyrrolidinium produced from acid-base reaction with host **2**. s: residual solvents.

Structural characterization of the inclusion complex 2⊃DMSO in solution

One single species is observed for the inclusion complex **2**⊃DMSO. We tested different solvents (*i.e.* $CDCl_3$, $(CDCl_2)_2$, and C_6D_6) to determine the best conditions to study this host–guest system (Figure S5). Even though the NMR signature of the **2**⊃DMSO complex is similar in all three solvents, we chose to proceed with C_6D_6 because CH_2 signals and *t*Bu signals were the most dispersed in this solvent rendering the structural and conformational characterization simpler.

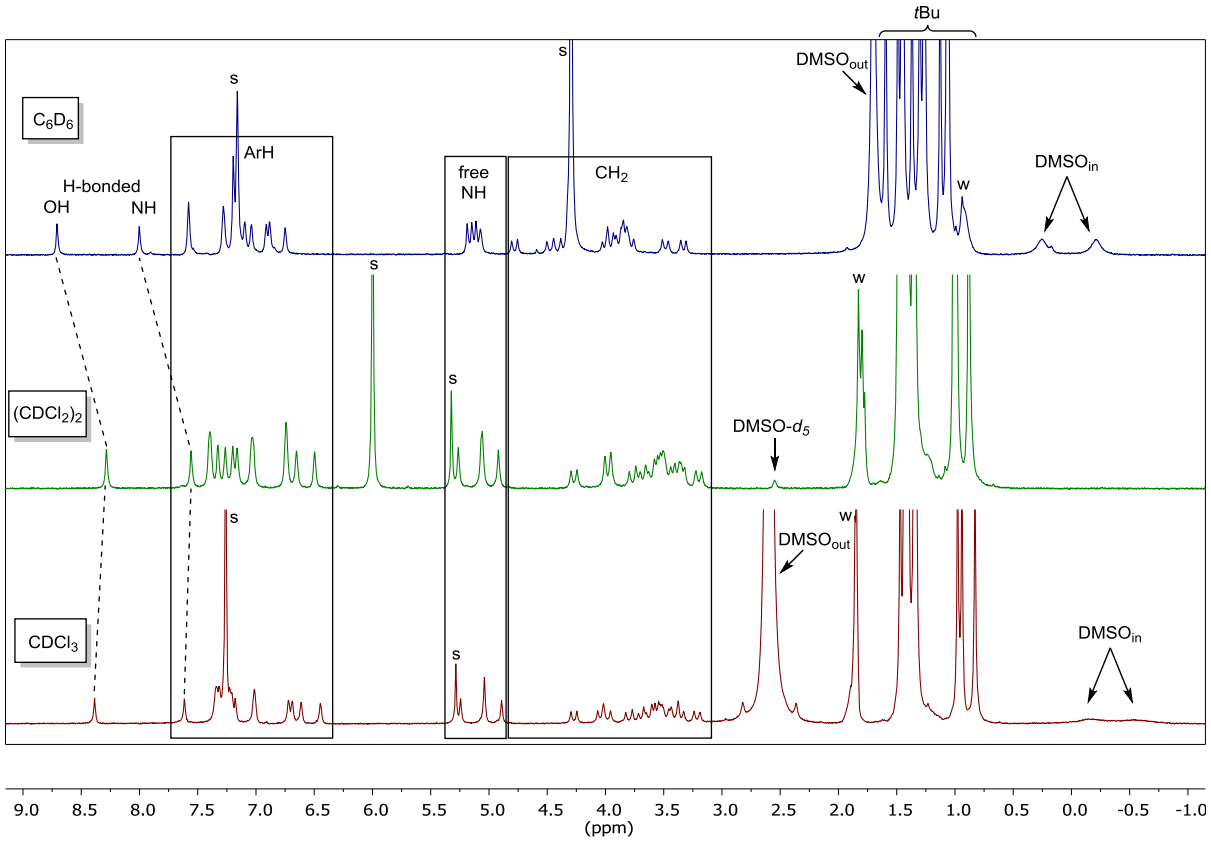

Figure S5. ^{1}H NMR spectra of **2**⊃DMSO complex in different solvents (300 MHz, 298 K). s: residual solvents. w: water. Note: an excess of DMSO was added in $CDCl_3$ and C_6D_6 while an excess of DMSO-d_6 was added in $(CDCl_2)_2$.

The following data set was previously published for host **2** structure characterization purpose.[1] The calixarene-based host **2** adopts an asymmetric conformation upon complexation of DMSO resulting in a high number of NMR signals. NMR signals assignment could nevertheless be achieved through exhaustive analysis of 2D spectra (dqfCOSY, edited HSQC, HMBC and ROESY spectra). The entire data set characterizing the inclusion complex **2**⊃DMSO is given in Tables S8-S13. Each table is referring to a single aromatic unit of this complex. The notations used for the assignment are defined in Figure S6; the spectra are shown in Figures S7.

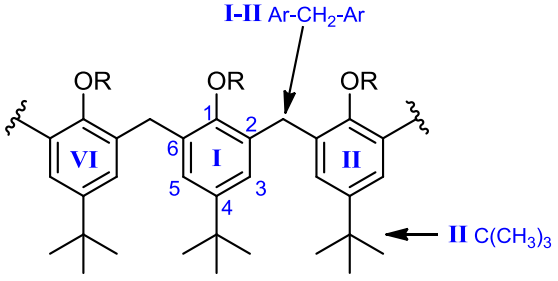

Figure S6: Notations used in Tables S8-S13.

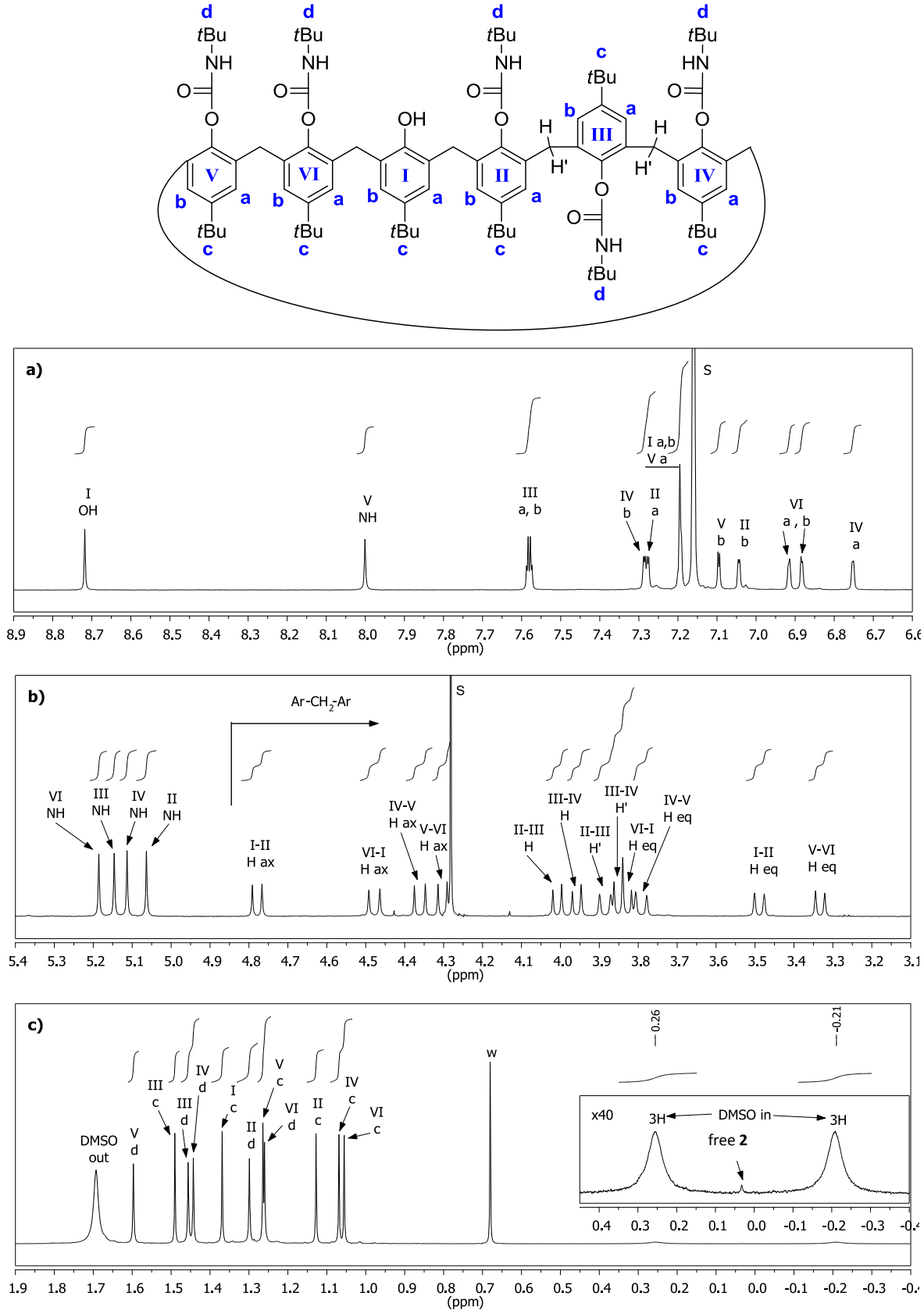

Figure S7. Assignment of the ^{1}H NMR spectrum of **2**⊃DMSO (600 MHz, C_6D_6/DMSO (99:1, v/v), 298 K). S: residual solvents, w: residual water. "H ax" and "H eq" refer respectively to the axial and equatorial hydrogen atoms of the methylene bridges.

Table S8: NMR analysis of **2**⊃DMSO complex (C_6D_6, 298K, 600 MHz) - **Unit I**

Group		δ ^{1}H (ppm)	M	J (Hz)	δ ^{13}C (ppm)	Cor, HMBC 8Hz #
VI-I	$ArCH_2Ar$ ax	4.48	d	16.8	29.6	^{2}J : Ar-C6 ^{3}J : Ar-C1 ; Ar-C5
VI-I	$ArCH_2Ar$ eq	3.88	d	16.8	29.6	^{2}J : Ar-C6 ^{3}J : Ar-C1 ; Ar-C5
I	Ar-OH	8.72	s	-	-	^{2}J : Ar-C1 ^{3}J : Ar-C6 ^{4}J : Ar-C3
I	Ar-C1	-	-	-	150.7	-
I	Ar-C2	-	-	-	136.2	-
I	Ar-C3H	7.19	n.d.	n.d.	128.2	^{2}J : *Ar-C2* ^{3}J : Ar-C1 ; Ar-C5 ; Ar-tBu C ; I-II $ArCH_2Ar$
I	Ar-C4	-	-	-	141.5	-
I	Ar-C5H	7.19	n.d.	n.d.	128.9	^{2}J : *Ar-C6* ^{3}J : Ar-C1 ; Ar-C3 ; Ar-tBu C ; VI-I $ArCH_2Ar$
I	Ar-C6	-	-	-	123.4	-
I	Ar-tBu C	-	-	-	34.2	-
I	Ar-tBu CH_3	1.37	s	-	31.8	^{2}J : Ar-tBu C ^{3}J : Ar-tBu CH_3, Ar-C4
I-II	$ArCH_2Ar$ ax	4.78	d	15.0	30.6	^{2}J : Ar-C2 ^{3}J : Ar-C1 ; Ar-C3
I-II	$ArCH_2Ar$ eq	3.49	d	15.0	30.6	^{2}J : Ar-C2 ^{3}J : Ar-C1 ; Ar-C3

M: multiplicity ; s: singlet ; d: doublet ; n.d.: not determined (signal overlapping).
The HMBC correlations imply a ^{13}C from unit I. Correlations of low intensity are in italic.

dqfCOSY correlations

Group		Group		type
VI-I	$ArCH_2Ar$ ax	**VI-I**	$ArCH_2Ar$ eq	^{2}J
I	Ar-C3H	**VI-I**	$ArCH_2Ar$ eq	^{4}J/^{6}J
I	Ar-C5H superposition	**I-II**	$ArCH_2Ar$ ax	^{4}J/^{6}J
		I-II	$ArCH_2Ar$ eq	^{4}J/^{6}J
I-II	$ArCH_2Ar$ ax	**I-II**	$ArCH_2Ar$ eq	^{2}J

ROESY correlations

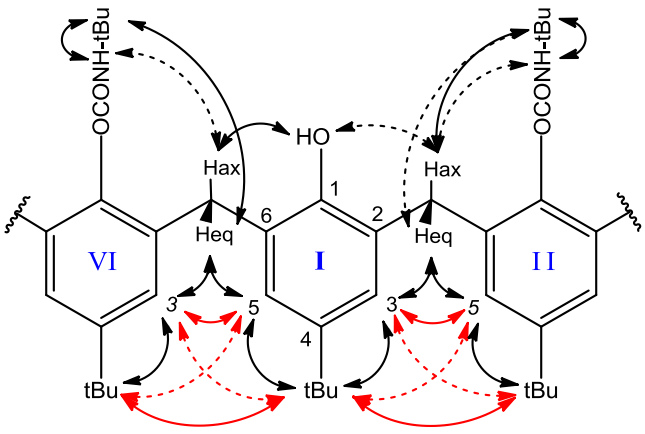

dqfCOSY correlations of very low intensity are in italic.
ROESY correlations of low intensity are dashed.
ROESY correlations in red characterize the relative orientation of adjacent units.

Table S9: NMR analysis of **2**⊃DMSO complex (C_6D_6, 298K, 600 MHz) - **Unit II**

Group		δ ^{1}H (ppm)	M	J (Hz)	δ ^{13}C (ppm)	Cor, HMBC 8Hz #
I-II	$ArCH_2Ar$ ax	4.78	d	15.0	30.6	^{3}J : Ar-C1 ; Ar-C5
I-II	$ArCH_2Ar$ eq	3.49	d	15.0	30.6	*^{2}J : Ar-C6* ^{3}J : Ar-C1 ; *Ar-C5*
II	Bac CH_3	1.30	s	-	28.5	^{2}J : Bac C ^{3}J : Bac CH_3
II	Bac C	-	-	-	50.3	-
II	Bac NH	5.06	s	-	-	^{2}J : Bac C ^{3}J : Bac CH_3
II	Bac CO	-	-	-	-	-
II	Ar-C1	-	-	-	146.5	-
II	Ar-C2	-	-	-	132.5 or 133.8*	-
II	Ar-C3H	7.28	d	1.8	126.1	^{3}J : Ar-C1 ; Ar-C5 ; Ar-tBu C ; II-III $ArCH_2Ar$
II	Ar-C4	-	-	-	146.7	-
II	Ar-C5H	7.04	d	1.8	124.5	^{3}J : Ar-C1 ; Ar-C3 ; Ar-tBu C ; I-II $ArCH_2Ar$
II	Ar-C6	-	-	-	132.4	-
II	Ar-tBu C	-	-	-	34.2	-
II	Ar-tBu CH_3	1.13	s	-	31.8	^{2}J : Ar-tBu C ^{3}J : Ar-tBu CH_3, Ar-C4
II-III	$ArCH_2Ar$ H	4.01	d	13.2	36.0	^{2}J : Ar-C2 ^{3}J : Ar-C1 ; Ar-C3
II-III	$ArCH_2Ar$ H’	3.85	d	13.2	36.0	^{2}J : Ar-C2 ^{3}J : Ar-C1 ; Ar-C3

M: multiplicity ; s: singlet ; d: doublet.

The HMBC correlations imply a ^{13}C from unit I. Correlations of low intensity are in italic.

* Undetermined.

dqfCOSY correlations

Group		Group		type
I-II	$ArCH_2Ar$ ax	**I-II**	$ArCH_2Ar$ eq	^{2}J
II	Ar-C5H	***I-II***	*$ArCH_2Ar$ ax*	*^{4}J*
		I-II	$ArCH_2Ar$ eq	^{4}J
		II-III	*$ArCH_2Ar$ H*	*^{6}J*
II	Ar-C3H	***II-III***	*$ArCH_2Ar$ H*	*^{4}J*
		II-III	$ArCH_2Ar$ H’	^{4}J
		I-II	$ArCH_2Ar$ eq	^{6}J
II	Ar-C5H	**II**	Ar-C3H	^{4}J
II-III	$ArCH_2Ar$ H	**II-III**	$ArCH_2Ar$ H’	^{2}J

ROESY correlations

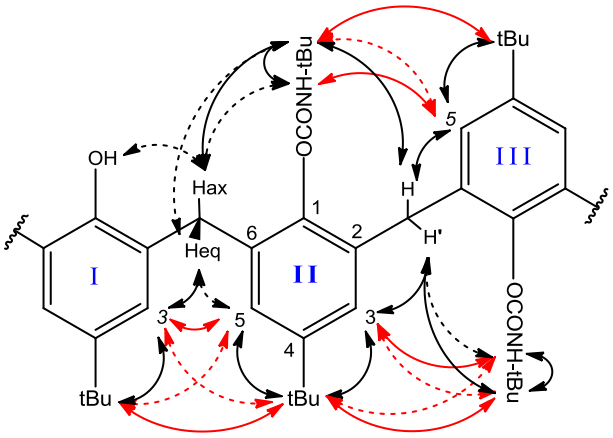

dqfCOSY correlations of very low intensity are in italic.

ROESY correlations of low intensity are dashed.

ROESY correlations in red characterize the relative orientation of adjacent units.

Table S10: NMR analysis of **2**⊃DMSO complex (C_6D_6, 298K, 600 MHz) - **Unit III**

Group		δ ^{1}H (ppm)	M	J (Hz)	δ ^{13}C (ppm)	Cor, HMBC 8Hz #
II-III	$ArCH_2Ar$ H	4.01	d	13.2	36.0	^{2}J : Ar-C6 ^{3}J : Ar-C1 ; Ar-C5
II-III	$ArCH_2Ar$ H'	3.85	d	13.2	36.0	^{2}J : Ar-C6 ^{3}J : Ar-C1 ; Ar-C5
III	Bac CH_3	1.46	s	-	29.0	^{2}J : Bac C ^{3}J : Bac CH_3
III	Bac C	-	-	-	51.3	-
III	Bac NH	5.15	s	-	-	^{2}J : Bac C ^{3}J : Bac CH_3
III	Bac CO	-	-	-	-	-
III	Ar-C1	-	-	-	147.7	-
III	Ar-C2	-	-	-	133.2	-
III	Ar-C3H	7.58	d	2.4	128.2	*^{2}J : Ar-C2* ^{3}J : Ar-C1 ; Ar-C5 ; Ar-tBu C; III-IV $ArCH_2Ar$
III	Ar-C4	-	-	-	147.5	-
III	Ar-C5H	7.58	d	2.4	128.2	^{3}J : Ar-C1 ; Ar-C3 ; Ar-tBu C ; II-III $ArCH_2Ar$
III	Ar-C6	-	-	-	132.5 or 133.8*	-
III	Ar-tBu C	-	-	-	34.6	-
III	Ar-tBu CH_3	1.49	s	-	32.1	^{2}J : Ar-tBu C ^{3}J : Ar-tBu CH_3, Ar-C4
III-IV	$ArCH_2Ar$ H	3.96	d	13.2	36.1	^{2}J : Ar-C2 ^{3}J : Ar-C1 ; Ar-C3
III-IV	$ArCH_2Ar$ H'	3.83	d	13.2	36.1	^{2}J : Ar-C2 ^{3}J : Ar-C1 ; Ar-C3

M: multiplicity ; s: singlet ; d: doublet.

The HMBC correlations imply a ^{13}C from unit I. Correlations of low intensity are in italic.

* Undetermined.

dqfCOSY correlations

Group		Group		type
II-III	$ArCH_2Ar$ H	**II-III**	$ArCH_2Ar$ H'	^{2}J
III	Ar-C3H	**II-III**	$ArCH_2Ar$ H	^{4}J/^{6}J
III	Ar-C5H superposition	**II-III**	$ArCH_2Ar$ H'	^{4}J/^{6}J
		III-IV	$ArCH_2Ar$ H	^{4}J/^{6}J
		III-IV	$ArCH_2Ar$ H'	^{4}J/^{6}J
III-IV	$ArCH_2Ar$ H	**III-IV**	$ArCH_2Ar$ H'	^{2}J

ROESY correlations

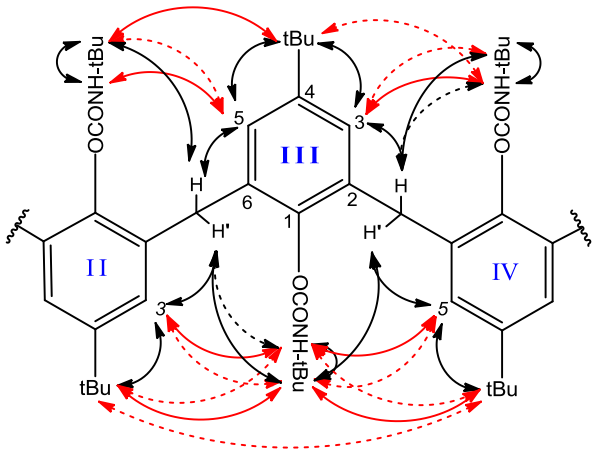

dqfCOSY correlations of very low intensity are in italic.

ROESY correlations of low intensity are dashed.

ROESY correlations in red characterize the relative orientation of adjacent units.

Table S11: NMR analysis of **2**⊃DMSO complex (C_6D_6, 298K, 600 MHz) - **Unit IV**

Group		δ ^{1}H (ppm)	M	J (Hz)	δ ^{13}C (ppm)	Cor, HMBC 8Hz #
III-IV	$ArCH_2Ar$ H	3.96	d	13.2	36.1	^{2}J : Ar-C6 ^{3}J : Ar-C1 ; Ar-C5
III-IV	$ArCH_2Ar$ H'	3.83	d	13.2	36.1	^{2}J : Ar-C6 ^{3}J : Ar-C1 ; Ar-C5
IV	Bac CH_3	1.44	s	-	28.8	^{2}J : Bac C ^{3}J : Bac CH_3
IV	Bac C	-	-	-	51.0	-
IV	Bac NH	5.11	s	-	-	^{2}J : Bac C ^{3}J : Bac CH_3
IV	Bac CO	-	-	-	-	-
IV	Ar-C1	-	-	-	146.6	-
IV	Ar-C2	-	-	-	134.4	-
IV	Ar-C3H	6.75	d	1.8	124.6	^{3}J : Ar-C1 ; Ar-C5 ; Ar-tBu C ; IV-V $ArCH_2Ar$ *^{4}J : Ar-C6*
IV	Ar-C4	-	-	-	146.8	-
IV	Ar-C5H	7.29	d	1.8	126.4	^{3}J : Ar-C1 ; Ar-C3 ; Ar-tBu C ; III-IV $ArCH_2Ar$ *^{4}J : Ar-C2*
IV	Ar-C6	-	-	-	132.8	-
IV	Ar-tBu C	-	-	-	34.2	-
IV	Ar-tBu CH_3	1.07	s	-	31.7	^{2}J : Ar-tBu C ^{3}J : Ar-tBu CH_3, Ar-C4
IV-V	$ArCH_2Ar$ ax	4.36	d	17.4	29.2	^{2}J : Ar-C2 ^{3}J : Ar-C1 ; Ar-C3 *^{4}J : Ar-C6*
IV-V	$ArCH_2Ar$ eq	3.79	d	17.4	29.2	^{2}J : Ar-C2 ^{3}J : Ar-C1 ; Ar-C3

M: multiplicity ; s: singlet ; d: doublet.

The HMBC correlations imply a ^{13}C from unit I. Correlations of low intensity are in italic.

dqfCOSY correlations

Group		Group		type
III-IV	$ArCH_2Ar$ H	**III-IV**	$ArCH_2Ar$ H'	^{2}J
IV	Ar-C5H	***III-IV***	*$ArCH_2Ar$ H*	*^{4}J*
		III-IV	*$ArCH_2Ar$ H'*	*^{4}J*
		IV-V	*$ArCH_2Ar$ ax*	*^{6}J*
		IV-V	$ArCH_2Ar$ eq	^{6}J
IV	Ar-C3H	**IV-V**	$ArCH_2Ar$ ax	^{4}J
		IV-V	$ArCH_2Ar$ eq	^{4}J
		III-IV	*$ArCH_2Ar$ H*	*^{6}J*
IV	Ar-C5H	**IV**	Ar-C3H	^{4}J
IV-V	$ArCH_2Ar$ ax	**IV-V**	$ArCH_2Ar$ eq	^{2}J

ROESY correlations

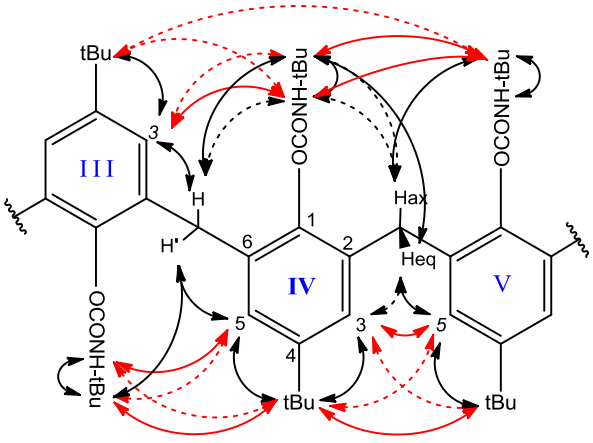

dqfCOSY correlations of very low intensity are in italic.

ROESY correlations of low intensity are dashed.

ROESY correlations in red characterize the relative orientation of adjacent units.

Table S12: NMR analysis of **2**⊃DMSO complex (C_6D_6, 298K, 600 MHz) - **Unit V**

Group		δ ^{1}H (ppm)	M	J (Hz)	δ ^{13}C (ppm)	Cor, HMBC 8Hz [#]
IV-V	$ArCH_2Ar$ ax	4.36	d	17.4	29.2	^{2}J : Ar-C6 ^{3}J : Ar-C1 ; Ar-C5
IV-V	$ArCH_2Ar$ eq	3.79	d	17.4	29.2	^{2}J : Ar-C6 ^{3}J : Ar-C1 ; Ar-C5
V	Bac CH_3	1.60	s	-	29.6	^{2}J : Bac C ^{3}J : Bac CH_3
V	Bac C	-	-	-	50.2	-
V	Bac NH	8.00	s	-	-	^{2}J : Bac C ^{3}J : Bac CH_3
V	Bac CO	-	-	-	-	-
V	Ar-C1	-	-	-	145.6	-
V	Ar-C2	-	-	-	135.9	-
V	Ar-C3H	7.19	n.d.	n.d.	126.5	^{3}J : Ar-C1 ; Ar-C5 ; Ar-tBu C ; V-VI $ArCH_2Ar$
V	Ar-C4	-	-	-	147.6	-
V	Ar-C5H	7.10	d	2.4	128.9	^{3}J : Ar-C1 ; Ar-C3 ; Ar-tBu C ; IV-V $ArCH_2Ar$
V	Ar-C6	-	-	-	131.2	-
V	Ar-tBu C	-	-	-	34.4	-
V	Ar-tBu CH_3	1.26	n.d.	-	31.7	^{2}J : Ar-tBu C ^{3}J : Ar-tBu CH_3, Ar-C4
V-VI	$ArCH_2Ar$ ax	4.30	d	14.4	31.6	^{2}J : Ar-C2 ^{3}J : Ar-C1 ; Ar-C3
V-VI	$ArCH_2Ar$ eq	3.33	d	14.4	31.6	^{2}J : Ar-C2 ^{3}J : Ar-C1 ; Ar-C3

M: multiplicity ; s: singlet ; d: doublet ; n.d.: not determined (signal overlapping).
[#] The HMBC correlations imply a ^{13}C from unit I. Correlations of low intensity are in italic.

dqfCOSY correlations

Group		Group		type
IV-V	$ArCH_2Ar$ ax	**IV-V**	$ArCH_2Ar$ eq	^{2}J
V	Ar-C5H	**IV-V** **V-VI**	$ArCH_2Ar$ eq $ArCH_2Ar$ ax	^{4}J ^{6}J
V	Ar-C3H	**V-VI** **V-VI** ***IV-V***	$ArCH_2Ar$ ax $ArCH_2Ar$ eq *$ArCH_2Ar$ eq*	^{4}J ^{4}J *^{6}J*
V	Ar-C5H	**V**	Ar-C3H	^{4}J
V-VI	$ArCH_2Ar$ ax	**V-VI**	$ArCH_2Ar$ eq	^{2}J

ROESY correlations

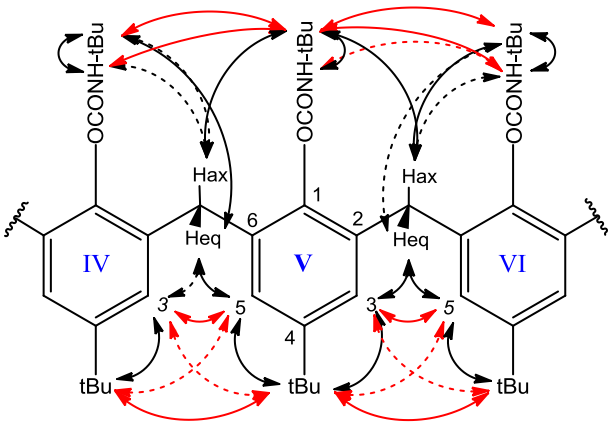

dqfCOSY correlations of very low intensity are in italic.
ROESY correlations of low intensity are dashed.
ROESY correlations in red characterize the relative orientation of adjacent units.

Table S13: NMR analysis of **2**⊃DMSO complex (C_6D_6, 298K, 600 MHz) - **Unit VI**

Group		δ ^{1}H (ppm)	M	J (Hz)	δ ^{13}C (ppm)	Cor. HMBC 8Hz #
V-VI	$ArCH_2Ar$ H	4.30	d	14.4	31.6	^{2}J : Ar-C6 ^{3}J : Ar-C1 ; Ar-C5
V-VI	$ArCH_2Ar$ H'	3.33	d	14.4	31.6	^{2}J : Ar-C6 ^{3}J : Ar-C1 ; Ar-C5
VI	Bac CH_3	1.26	n.d.	-	28.8	^{2}J : Bac C ^{3}J : Bac CH_3
VI	Bac C	-	-	-	50.7	-
VI	Bac NH	5.19	s	-	-	^{2}J : Bac C ^{3}J : Bac CH_3
VI	Bac CO	-	-	-	-	-
VI	Ar-C1	-	-	-	146.0	-
VI	Ar-C2	-	-	-	134.2	-
VI	Ar-C3H	6.92	d	1.8	122.9	^{3}J : Ar-C1 ; Ar-C5 ; Ar-tBu C ; VI-I $ArCH_2Ar$ *^{4}J : Ar-C6*
VI	Ar-C4	-	-	-	146.5	-
VI	Ar-C5H	6.88	d	1.8	124.6	^{3}J : Ar-C1 ; Ar-C3 ; Ar-tBu C ; V-VI $ArCH_2Ar$ *^{4}J : Ar-C2*
VI	Ar-C6	-	-	-	133.5	-
VI	Ar-tBu C	-	-	-	34.3	-
VI	Ar-tBu CH_3	1.06	s	-	31.6	^{2}J : Ar-tBu C ^{3}J : Ar-tBu CH_3, Ar-C4
VI-I	$ArCH_2Ar$ ax	4.48	d	16.8	29.6	^{3}J : Ar-C1 ; Ar-C3
VI-I	$ArCH_2Ar$ eq	3.88	d	16.8	29.6	^{3}J : Ar-C1 ; Ar-C3

M: multiplicity ; s: singlet ; d: doublet ; n.d.: not determined (signal overlapping).
The HMBC correlations imply a ^{13}C from unit I. Correlations of low intensity are in italic.

dqfCOSY correlations

Group		Group		type
V-VI	$ArCH_2Ar$ ax	**V-VI**	$ArCH_2Ar$ eq	^{2}J
VI	Ar-C5H	**V-VI** ***VI-I*** **VI-I**	$ArCH_2Ar$ eq *$ArCH_2Ar$ ax* $ArCH_2Ar$ eq	^{4}J *^{6}J* ^{6}J
VI	Ar-C3H	**VI-I** **VI-I** **V-VI**	$ArCH_2Ar$ ax $ArCH_2Ar$ eq $ArCH_2Ar$ eq	^{4}J ^{4}J ^{6}J
VI	Ar-C5H	**VI**	Ar-C3H	^{4}J
VI-I	$ArCH_2Ar$ ax	**VI-I**	$ArCH_2Ar$ eq	^{2}J

ROESY correlations

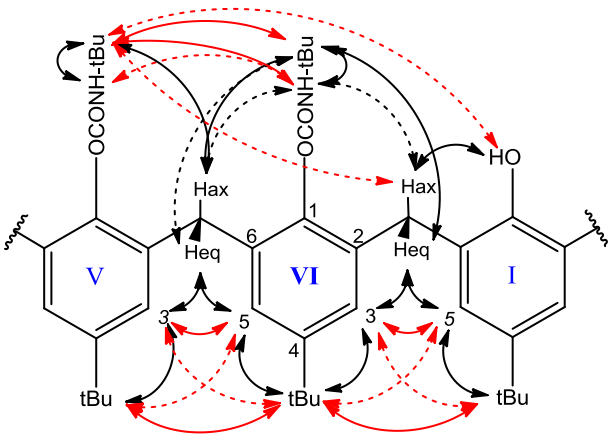

dqfCOSY correlations of very low intensity are in italic.
ROESY correlations of low intensity are dashed.
ROESY correlations in red characterize the relative orientation of adjacent units.

Structural characterization of the inclusion complex 2⊃imidazole in solution

Similarly to the DMSO inclusion complex **2**⊃DMSO (*vide supra*), the exhaustive analysis of the imidazole inclusion complex **2**⊃imidazole by 1D and 2D NMR spectroscopy led to the complete assignment of the ^{1}H and ^{13}C NMR signals and revealed that the calixarenic host **2** adopts a similar conformation with a single inverted unit III.

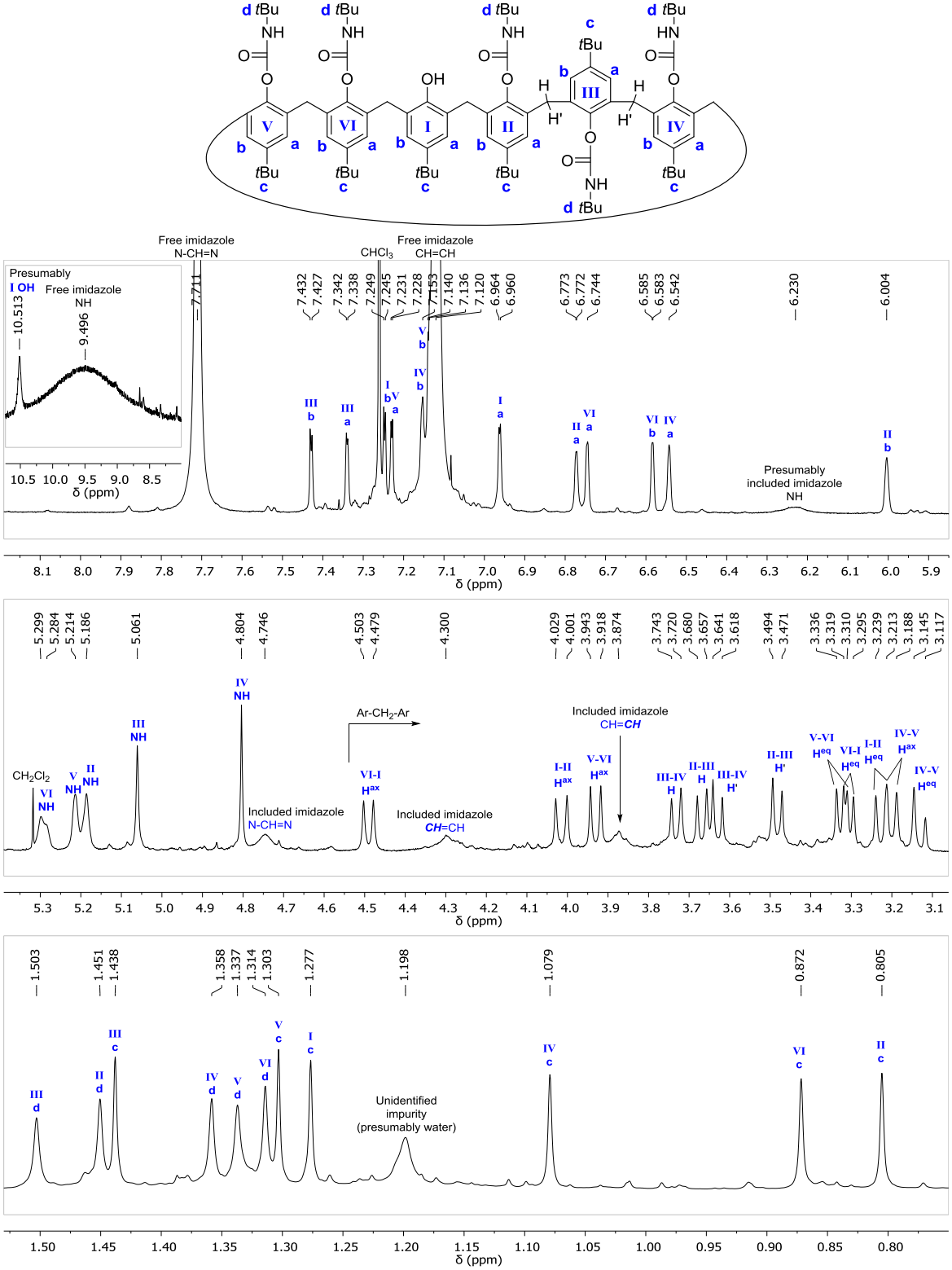

Figure S14. Assignment of the ^{1}H NMR spectrum of **2**⊃imidazole (600 MHz, $CDCl_3$, 223 K). "H^{ax}" and "H^{eq}" refer respectively to the axial and equatorial hydrogen atoms of the methylene bridges.

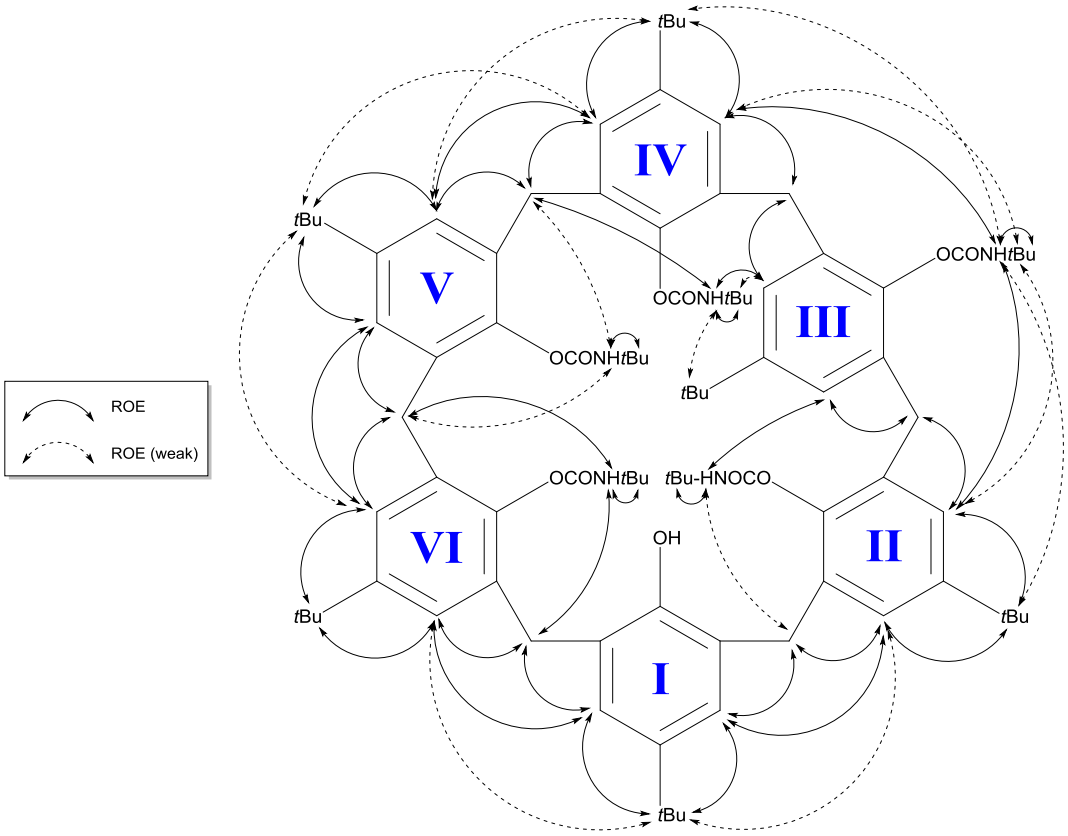

Figure S15. ROE correlations for the calixarenic part of **2**⊃imidazole (600 MHz, $CDCl_3$, 223 K). See ROESY spectrum in Figure S20. The ROE correlations observed are consistent with the inversion of unit III.

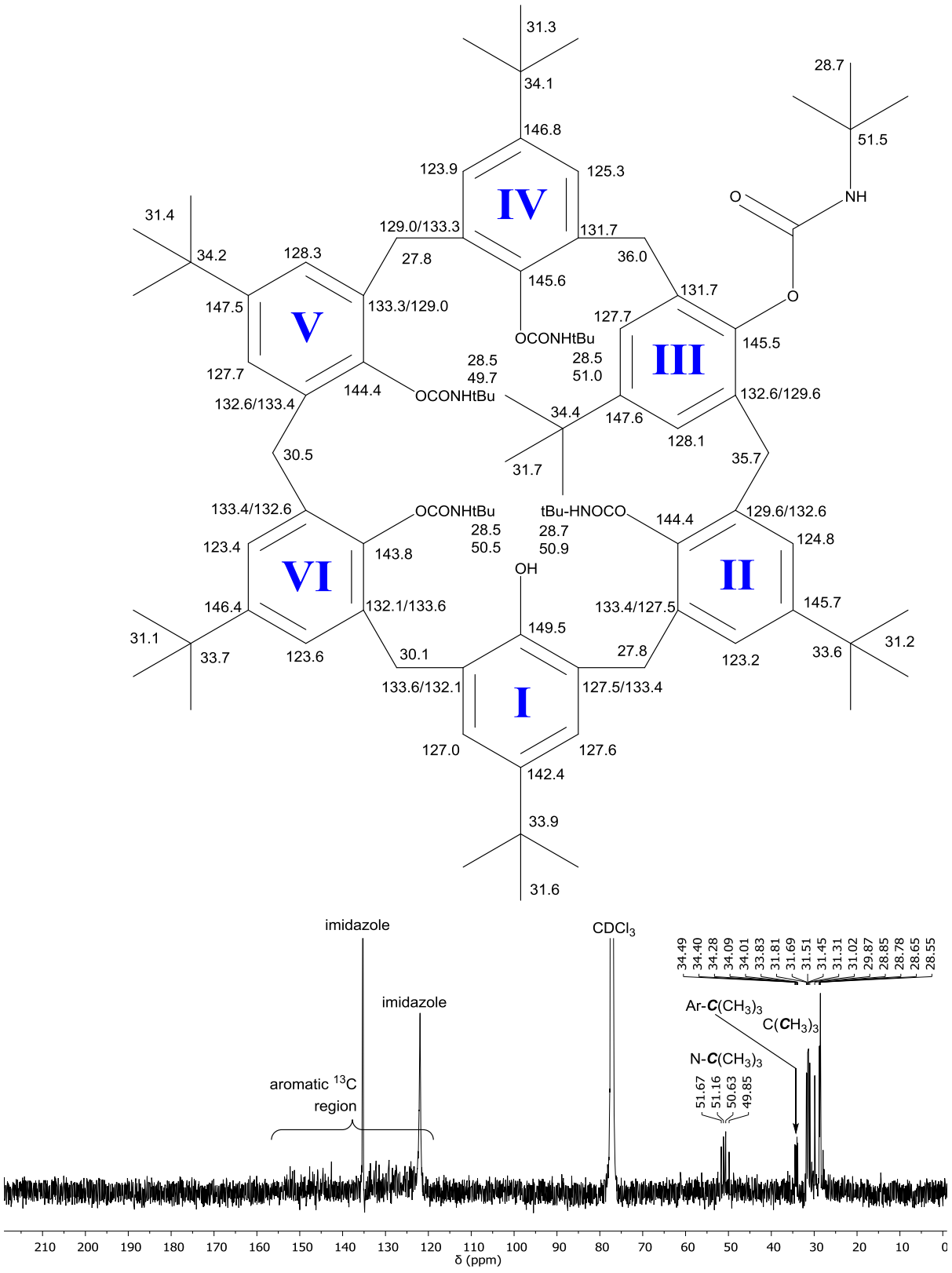

Figure S16. ^{13}C NMR spectrum of **2**⊃imidazole (151 MHz, $CDCl_3$, 223 K, 10110 scans) and assigned structure. Despite the high number of scans, the aryl and carbonyl signals are too weak to be observed clearly, thus the assignment is based on the HSQC and HMBC spectra (Figures S18 and S19). Uncertainty is still present between C^2 and C^6 carbons on the aryl units, thus the two potential values are provided.

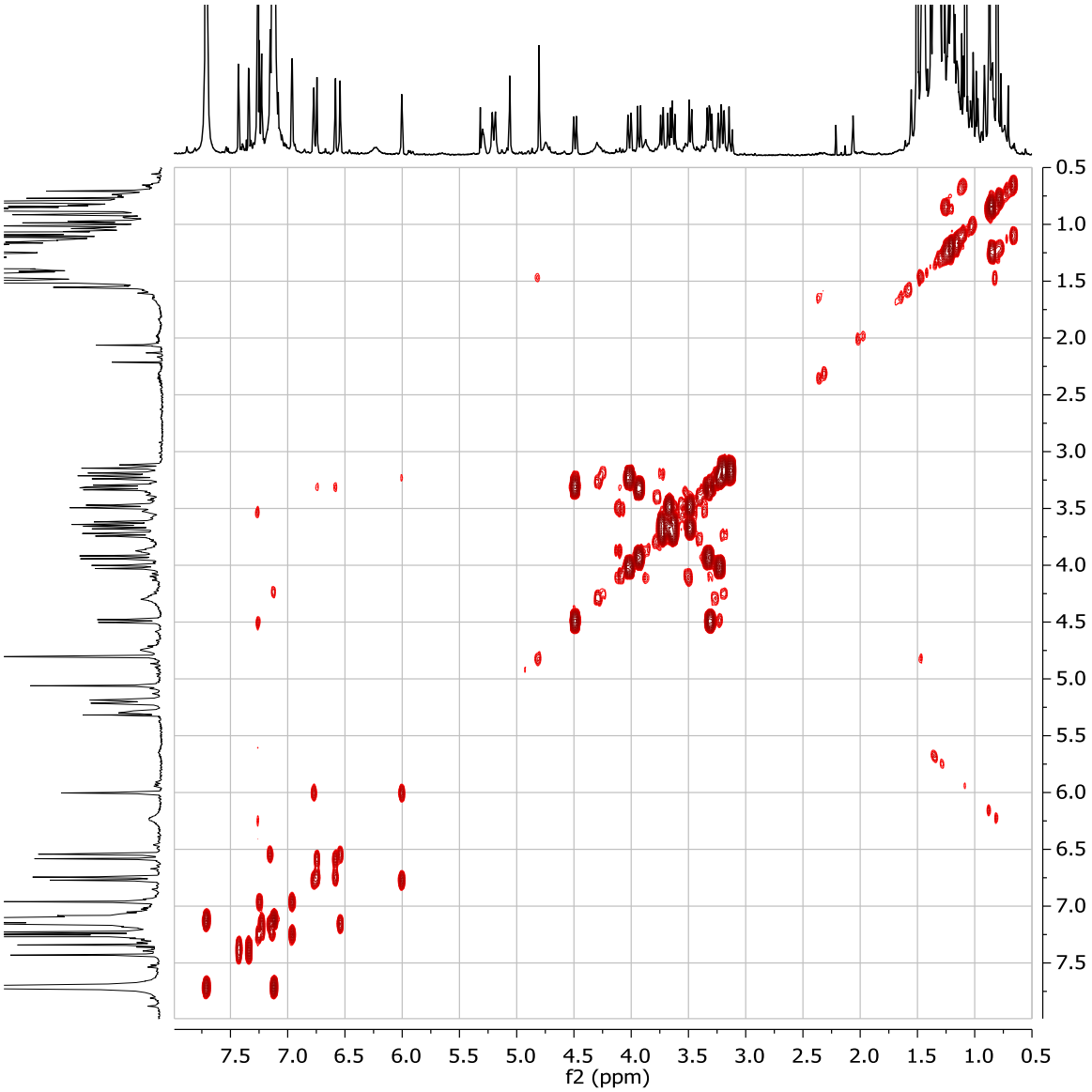

Figure S17. dqfCOSY spectrum of **2**⊃imidazole (600 MHz, $CDCl_3$, 223 K).

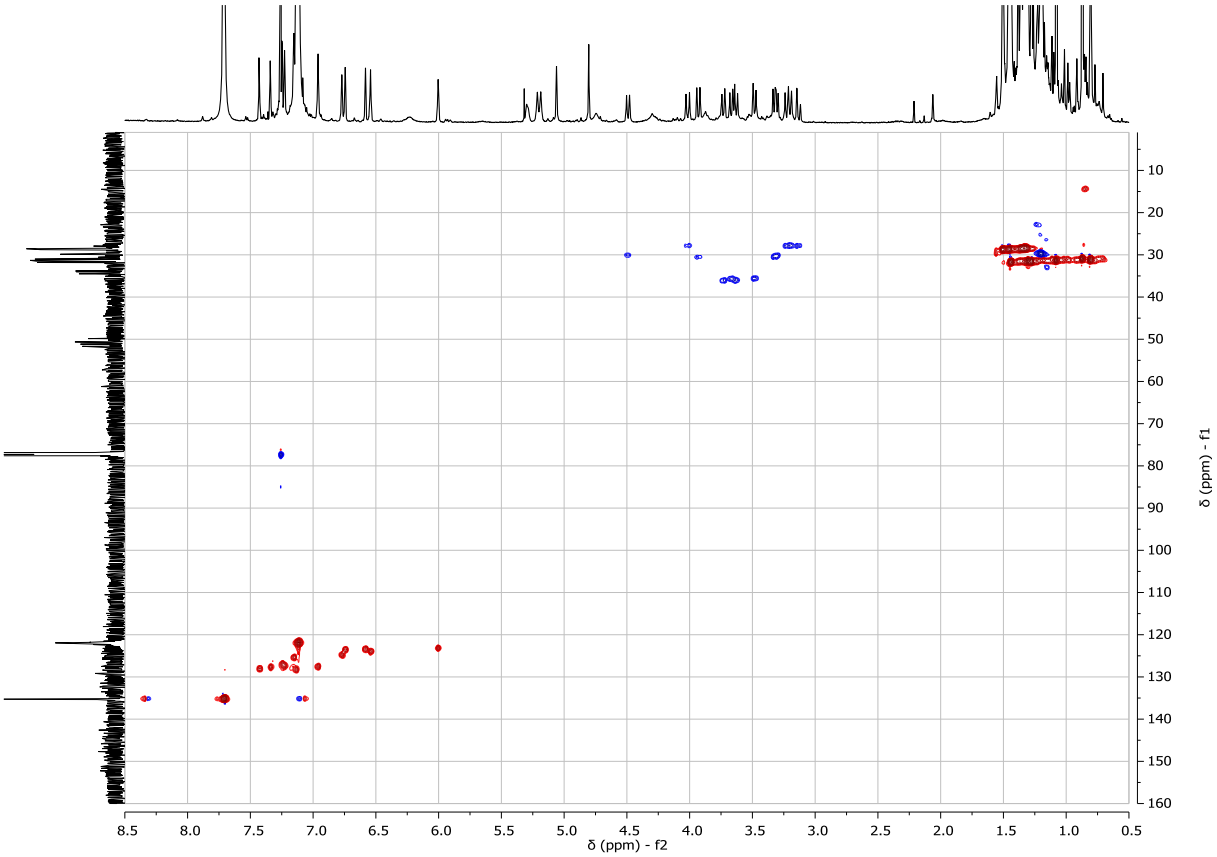

Figure S18. Edited ^{1}H-^{13}C HSQC spectrum of **2**⊃imidazole (14.1 Tela, $CDCl_3$, 223 K).

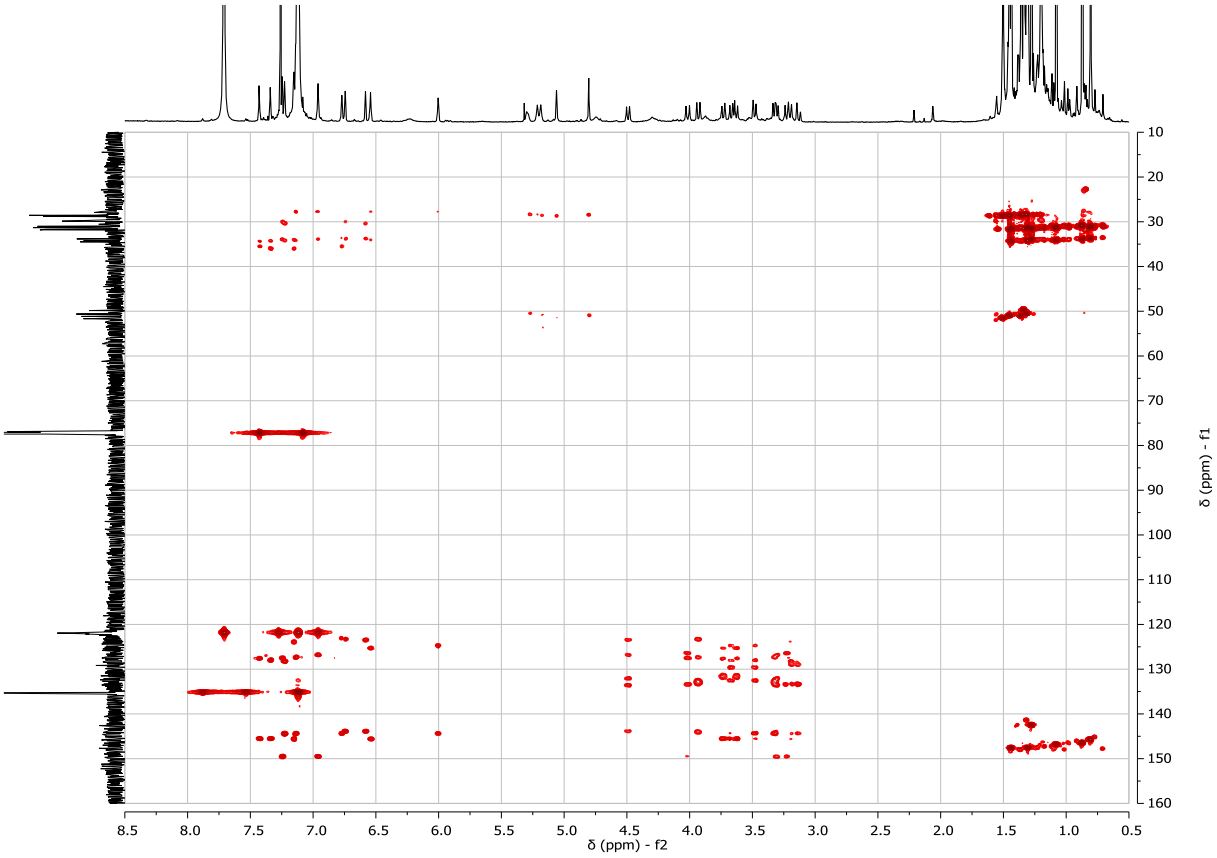

Figure S19. ^{1}H-^{13}C HMBC spectrum of **2**⊃imidazole (8 Hz, 14.1 Tesla, $CDCl_3$, 223 K).

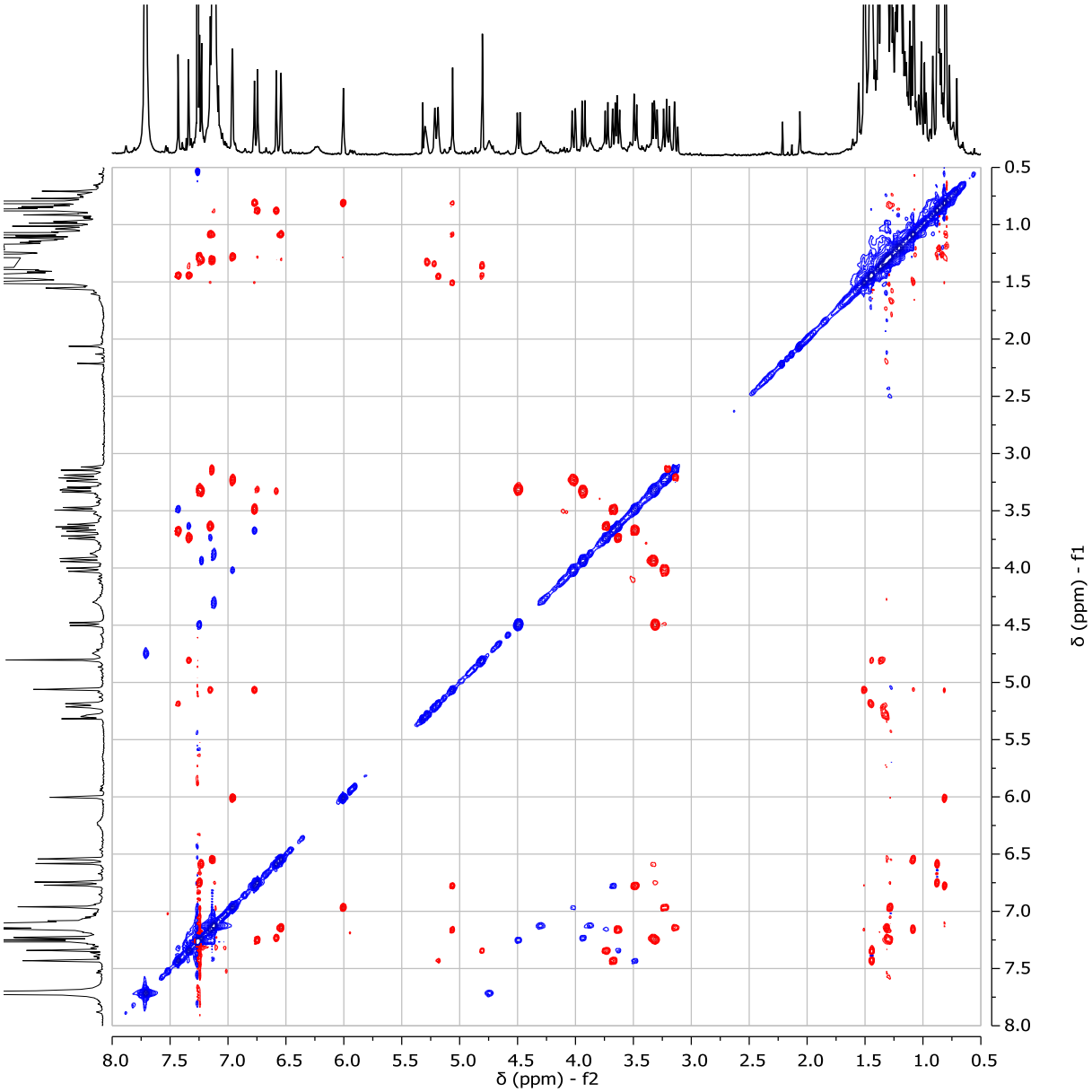

Figure S20. Symmetrized ROESY spectrum of **2**⊃imidazole (τ_m: 400 ms, 600 MHz, $CDCl_3$, 298 K). Red spots correspond to ROE correlations. Off-diagonal blue spots correspond to either EXSY correlations or indirect ROE's (three-spin effects).

Structural characterization of the inclusion complex 2⊃Imi in solution

The addition of an excess of 2-imidazolidinone (Imi) to calixarene **2** in $CDCl_3$ leads to host-guest complexes. One predominant species arises and was identified to a 1:1 inclusion complex **2**⊃Imi by NMR spectroscopy. The ^{1}H NMR spectrum presents numerous signals which indicates that the calixarenic host adopts an asymmetric conformation similarly to other inclusion complexes characterized herein. The presence of secondary peaks of intensity *ca.* 20% of the peaks of the major complex indicates that other host-guest complexes are also formed which might correspond to different conformers of the host, exo-complexation and/or different stoichiometries of host and guest. The overlapping of peaks corresponding to the different species in solution limits our ability to further characterize the structure, conformation and to provide full assignment. The NMR spectra are shown below.

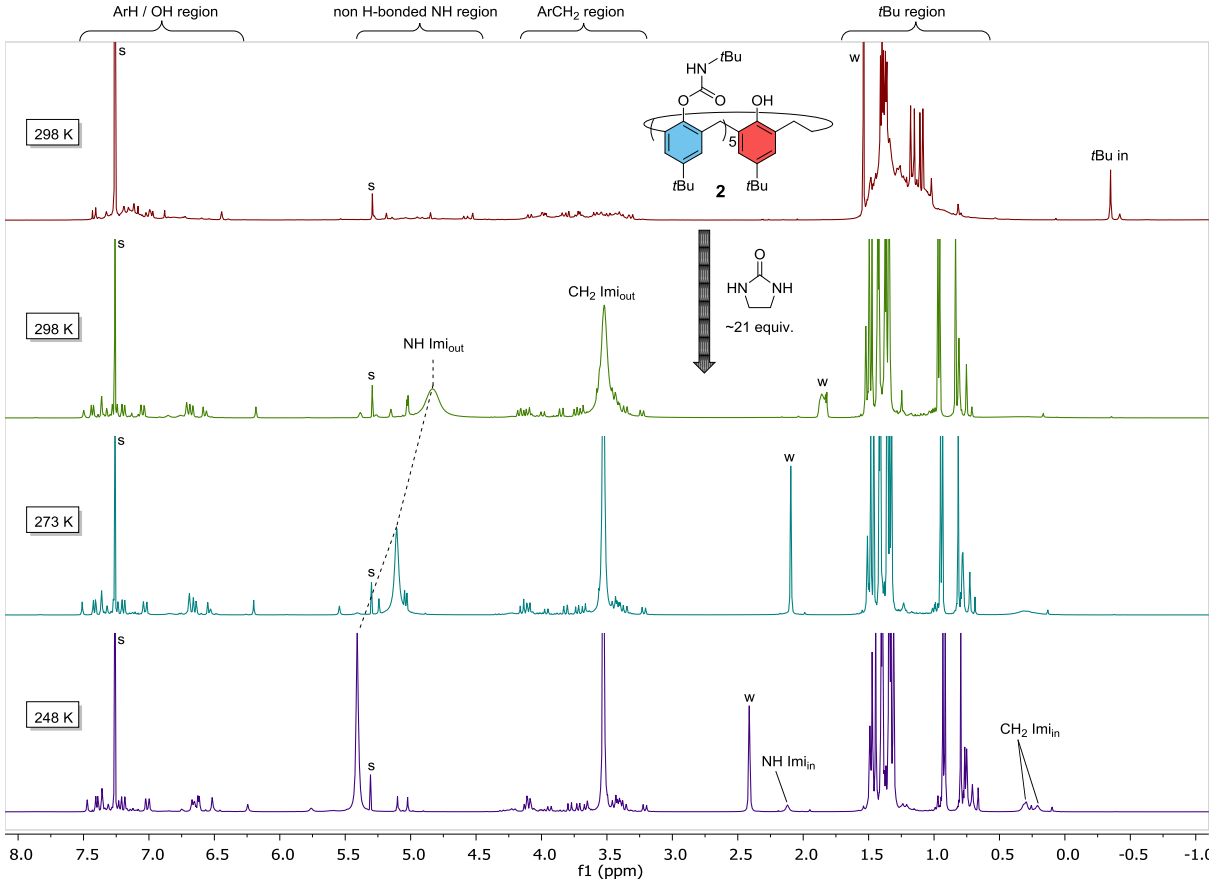

Figure S21. ^{1}H NMR spectra of **2** and **2**⊃Imi inclusion complexes at different temperatures (600 MHz, $CDCl_3$). s: residual solvents; w: residual water. Despite showing one major **2**⊃Imi species, peaks of smaller intensity are observed and were attributed to at least one different **2**⊃Imi complex based on EXSY correlations observed in a 2D-ROESY spectrum (see Figure S24).

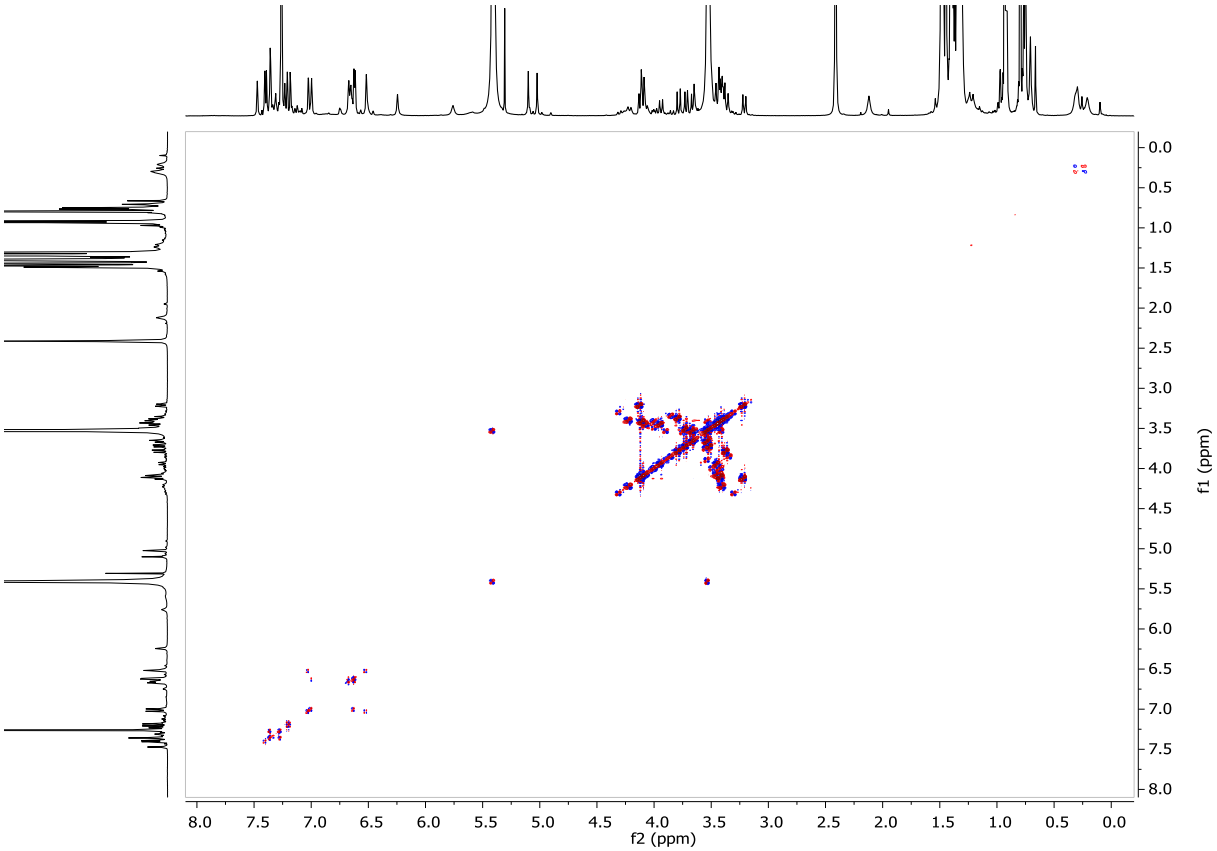

Figure S22. dqfCOSY spectrum of **2**⊃Imi (600 MHz, $CDCl_3$, 248 K).

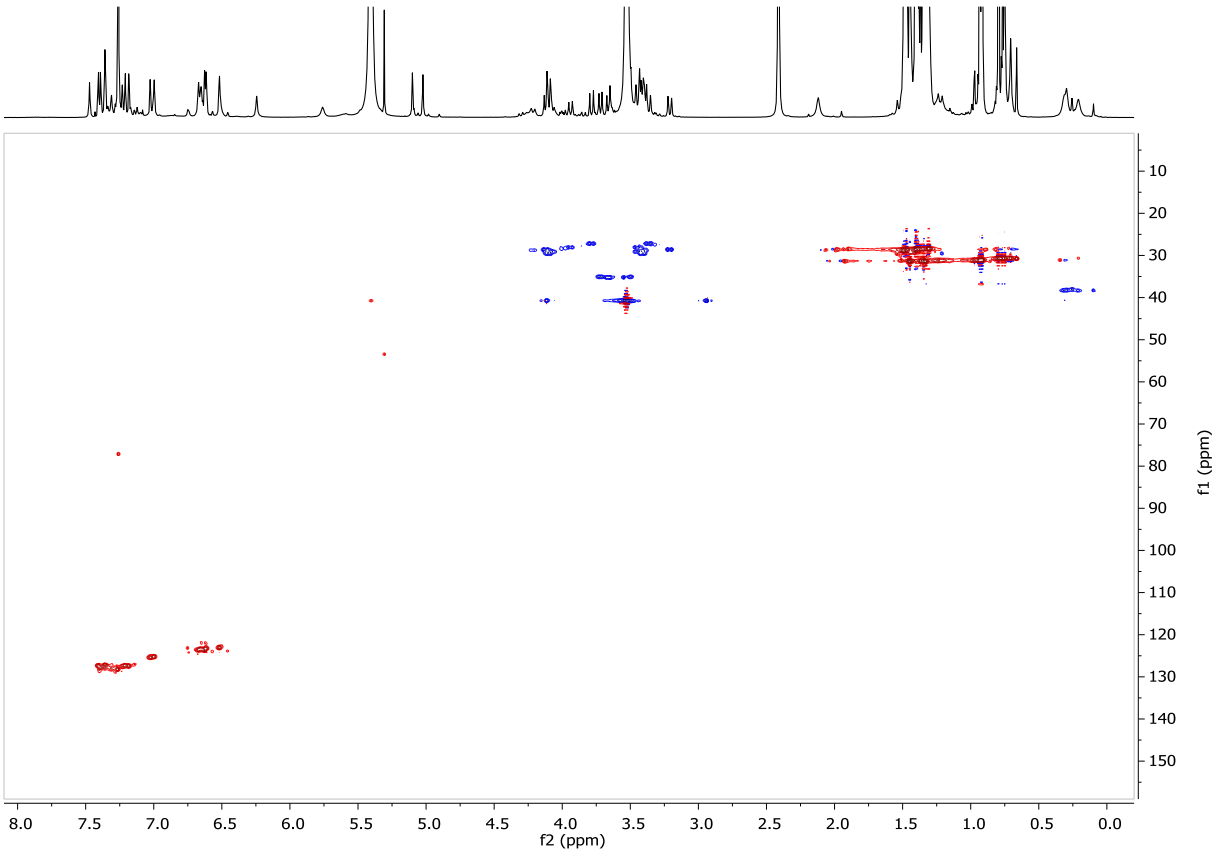

Figure S23. Edited ^{1}H-^{13}C HSQC spectrum of **2**⊃Imi (14.1 Tesla, $CDCl_3$, 248 K).

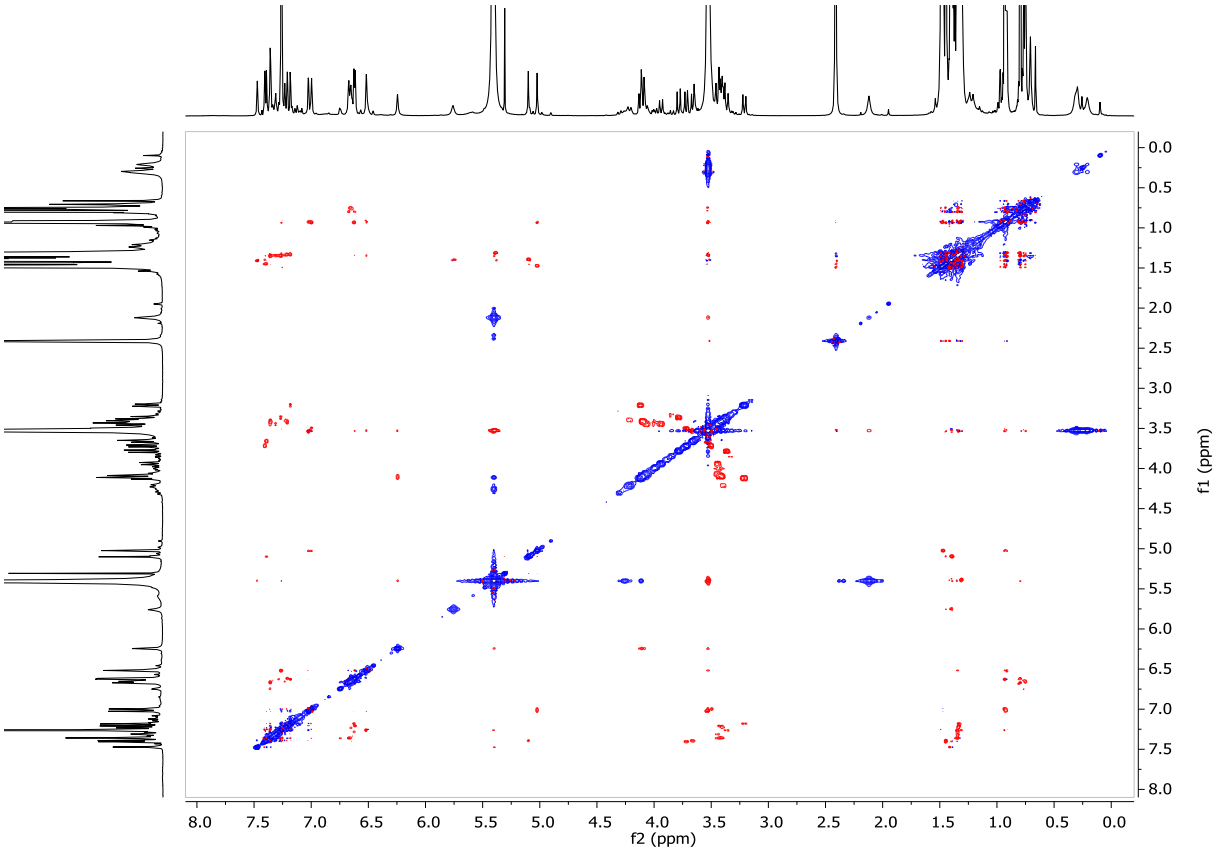

Figure S24. Symmetrized ROESY spectrum of **2**⊃Imi (τ_m: 300 ms, 600 MHz, $CDCl_3$, 298 K). ROE correlations are in red. EXSY correlations are in blue.

Determination of association constants

Inclusion complex **2**⊃DMSO

The in-out DMSO exchange for **2**⊃DMSO is slow on the chemical shift time scale in C_6D_6 (^{1}H, 600 MHz, 298 K). Thus we can integrate signals for the free host (H), the free guest (G) and the complex (HG) and calculate the association constant K_a following the equation

$$K_a = \frac{[\mathrm{HG}]}{[\mathrm{H}] \times [\mathrm{G}]}$$

This could be done in a single spectrum. Nevertheless, we proceeded with a titration to increase the accuracy and calculating the K_a for each titration point. The averaged value and relative error are K_a = 4.6×10^3 M^{-1} ±11%. The relative error corresponds to the standard deviation.

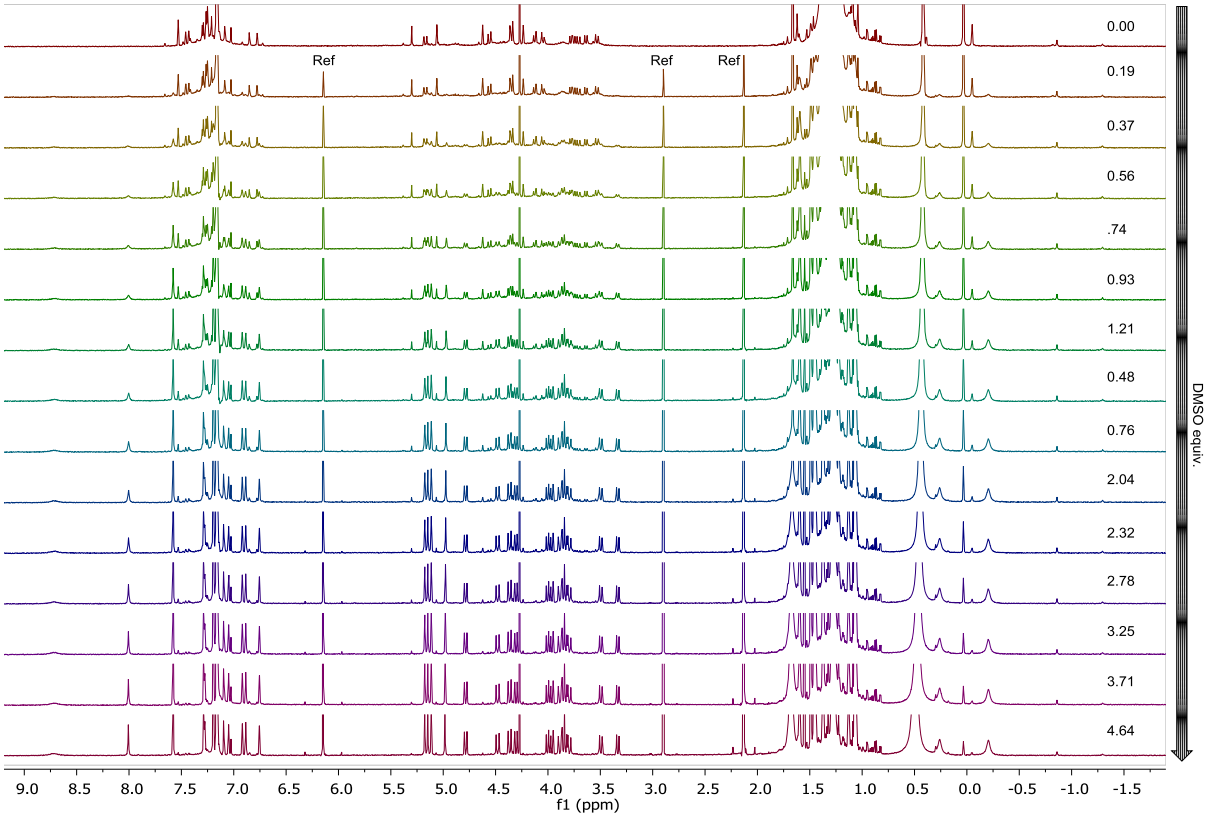

Figure S25. ^{1}H NMR spectra (600 MHz, C_6D_6, 298 K) of the titration experiment to calculate association constant K_a between host **2** and DMSO. $[\mathbf{2}]_0$ = 5.5×10^{-4} M. Ref: internal references ($CHCl_3$, $(CH_2Cl)_2$ and hexamethylbenzene) added to a stock solution of DMSO.

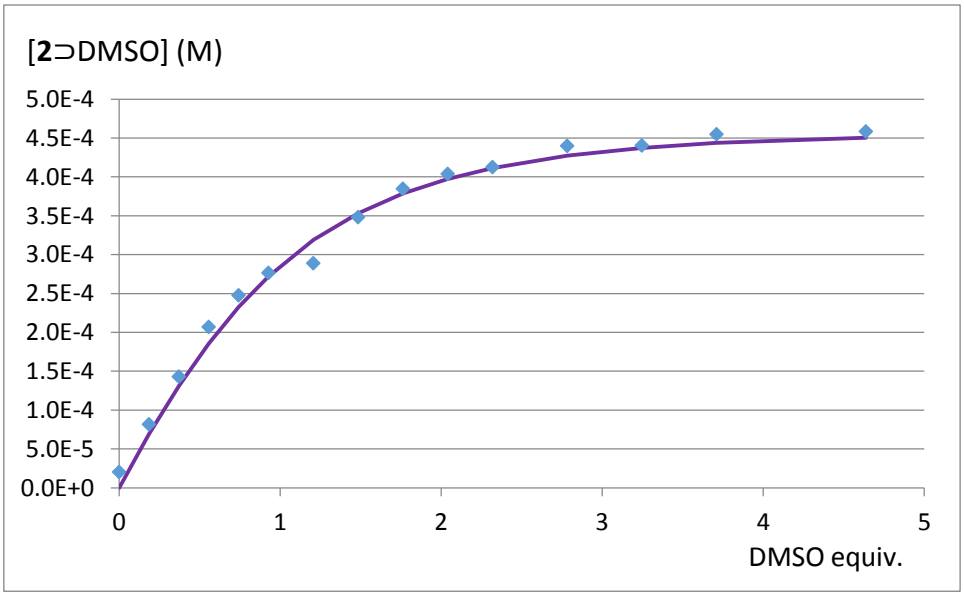

Figure S26. Titration curve for the formation of **2**⊃DMSO inclusion complex in C_6D_6 at 298 K ($[\mathbf{2}]_0$ = 5.5 × 10^{-4} M). Diamonds are experimental points. The curve is a simulation of the expected concentration of **2**⊃DMSO for the calculated association constant K_a = 4.6 × 10^3 M^{-1}.

The curve in Figure S26 for [**2**⊃DMSO] was simulated following the equations

$$K_a = \frac{[\mathrm{HG}]}{[\mathrm{H}] \times [\mathrm{G}]} = \frac{[\mathrm{HG}]}{([\mathrm{H}]_t - [\mathrm{HG}]) \times ([\mathrm{G}]_t - [\mathrm{HG}])}$$

=>

$$[\mathrm{HG}] = \frac{K_a \times [\mathrm{H}]_t + K_a \times [\mathrm{G}]_t + 1 - \sqrt{(K_a \times [\mathrm{H}]_t + K_a \times [\mathrm{G}]_t + 1)^2 - 4\,K_a^2 \times [\mathrm{H}]_t \times [\mathrm{G}]_t}}{2\,K_a}$$

Were $[H]_t$ and $[G]_t$ are the total concentration of host (**2**) and guest (DMSO) in solution, respectively.

Inclusion complex **2**⊃imidazole

The association constant was determined between **2** and imidazole in $CDCl_3$ at 298 K in a similar fashion to the aforementioned method at four different concentrations.

K_a = 208 M^{-1} ±13%

Inclusion complex **2**⊃thiazole

The association constant was determined between **2** and thiazole in $CDCl_3$ at 223 K in a similar fashion to the aforementioned method at four different concentrations.

K_a = 21 M^{-1} ±19%

X-ray crystallography of 2⊃DMSO

The single crystals of **2**⊃DMSO were obtained as blocks by slow evaporation at room temperature of a solution of **2** in $CHCl_2CHCl_2$/DMSO (1:1).

Single crystal X-ray data for **2**⊃DMSO were collected at 123 K on a Rigaku Oxford Diffraction SuperNova dual-source diffractometer equipped with an Atlas detector using mirror-monochromated Cu-Kα (λ = 1.54184 Å) radiation. The CrysAlisPro software[2] was used for data collection (*ω* scans) and processing. The structures were solved by intrinsic phasing method (SHELXT[3]) and refined by full-matrix least squares on F^2 using SHELXL[4] in the OLEX2 program package.[5] The crystals were quite strongly diffracting but the very severe disorder of the high electron count tetrachloroethane solvent molecules caused the final quality of the structure to be only moderate. All non-H atoms, except some of the *tert*-butyl methyl groups, of the structure were clearly established with SHELXT structure solution. All non-H atoms were refined anisotropically, yet the very severe, and unresolvable, disorder of the tetrachloroethane solvent molecules hampered the final refinements, and thus a moderate number (52) of restraints and constraints on the geometric and anisotropic displacement parameters were applied. All hydrogen atoms were refined using riding model. The DFIX restraints were used to ensure the chemical sensibility (bond lengths and angles) of some parts of the calixarene **2**. A few EADP constraints were used to restrict the ill-behaving thermal parameters of some of the *tert*-butyl methyl groups of the structure. The very severe disorder of the tetrachloroethane solvent molecules allowed the location and refinement of only one of them, the remaining scattered, yet high, electron density was removed by applying the solvent masking (aka SQUEEZE[6]) protocol within the OLEX2 program package.[5] The main details of the crystal data collection and refinement parameters are presented below. CCDC 1952601 (**2**⊃DMSO) contains the supplementary crystallographic data for this paper. These data can be obtained free of charge via https://www.ccdc.cam.ac.uk/structures

Crystal data: $C_{95}H_{137}N_5O_{12}SCl_4$, M = 1714.95, monoclinic, space group *Pn*, a = 16.8434(5), b = 14.3257(4), c = 25.5107(7) Å, α = 90, β = 92.891(3), γ = 90°, V = 6147.7(3) Å^3, Z = 2, ρ_{calc} = 0.926 Mgm^{-3}, μ = 1.401 mm^{-1}, $F(000)$ = 1844, θ range = 3.22 – 66.75°, 37196 reflections collected, 17170 unique (R_{int} = 0.0402), 11948 observed [$I>2\sigma(I)$], 922 parameters and 52 restraints, Goodness-of-fit (F^2) = 1.566. Final R indices [$I>2\sigma(I)$]: R_1 = 0.1541 and wR_2 = 0.3923. R indices (all data): R_1 = 0.1743 and wR_2 = 0.4222. Largest residual electron densities: 0.642 and –0.474 e Å^{-3}.

X-ray crystallography of 2

Single crystals of **2** were obtained from solutions in various chlorinated solvents (*i.e.* CH_2Cl_2, $CHCl_3$ and $(CHCl_2)_2$) by slow evaporation and/or by cooling to 253 K. Single crystals were also produced by diffusion of MeCN, MeOH or Et_2O in solutions of **2** in various chlorinated solvents (*i.e.* CH_2Cl_2, $CHCl_3$ $(CH_2Cl)_2$ and $(CHCl_2)_2$) at room temperature but their analysis is not discussed here.

Data collection using in-house sources

Single crystal X-ray data for **2** were collected either at 123 K on a Rigaku Oxford Diffraction SuperNova dual-source diffractometer equipped with an Atlas detector using mirror-monochromated Cu-Kα (λ = 1.54184 Å) radiation, or at 145 K on a Gemini Oxford Ruby diffractometer using Cu-Kα (λ = 1.54184 Å) radiation.

In all cases we observed a trigonal crystal system with $R\bar{3}$ space group. Unfortunately, the important orientational disorder of the calixarenic structure discussed in the main text and disordered solvent molecules rendered the refinement extremely challenging. R_1 > 0.20 were obtained in all cases limiting the extent of interpretable data. Therefore, these structures were not submitted to the CCDC database.

We provide below in Tables S27 and S28 the atom coordinates of non-hydrogen atoms for the disordered structure of **2** and the single orientation of **2** deduced from the disordered structure as presented in Figure 2 of the main text. These coordinates correspond to the best data we could obtain using in-house sources with single crystals grown from a solution in $CHCl_3$. The Cartesian coordinates given below can be pasted in a text file with .xyz extension.

Data collection with synchrotron radiation

Better quality data was obtained post-peer-review using synchrotron radiation with crystals of **2** obtained by cooling a solution of **2** in $CHCl_3$ to 253 K overnight. The unit cell and orientational disorder were consistent with the structures obtained using in-house sources.

Data were collected at Beamline I19 of the Diamond Light Source employing silicon double crystal monochromated synchrotron radiation (0.6889 Å) with ω and ψ scans at 100(2) K.[7] Data integration and reduction were performed using Xia2.[8]

The structure was solved by intrinsic phasing method (SHELXT[3]) and refined by full-matrix least squares against F^2 using SHELXL[4] within the OLEX2[5] and WinGX[9] program environments. All non-H atoms were refined anisotropically. All hydrogen atoms were refined using riding model. The asymmetric unit was found to contain 1/6 of the molecule of **2**, suggesting the disorder of the free phenol subunit as a minor component over all 6 subunits of **2**. The free phenol subunit could be identified from the residual electron density and modeled with the fixed occupancy of 1/6 with the occupancy of the carbamated subunit fixed at 5/6. Bond length restraints were applied to ensure the sensible geometry of both disorder components, with the planarity restraints additionally applied to the minor component only. Rigid-body and proximity restraints were also applied to the anisotropic displacement parameters. Furthermore, a small twin component was identified, related to the main twin component by a two-fold rotation (with the operator 0 1 0 1 0 0 0 0 −1), with its batch scale factor refining to 0.0103(10). Finally, the solvent encapsulated inside the cavity of **2** could not be identified or modeled and its contribution to the structure factors was accounted for using the SQUEEZE[6] procedure as implemented in PLATON[10]. The main details of the crystal data collection and refinement parameters are presented below. CCDC 1959492 contains the supplementary

crystallographic data for this paper. These data can be obtained free of charge via https://www.ccdc.cam.ac.uk/structures

Crystal data: $C_{97}H_{135}Cl_{18}N_5O_{11}$, M = 2185.19, trigonal, space group $R\bar{3}$, a = b = 28.1030(3), c = 13.4199(2) Å, α = 90, β = 120, γ = 90°, V = 9178.83(16) Å^3, Z = 3, ρ_{calc} = 1.186 Mgm^{-3}, μ = 0.418 mm^{-1}, F(000) = 3438, θ range = 1.680 – 24.977°, 13177 reflections collected, 3077 unique (R_{int} = 0.0831), 1910 observed [$I>2\sigma(I)$], 315 parameters and 802 restraints, Goodness-of-fit (F^2) = 1.285. Final R indices [$I>2\sigma(I)$]: R_1 = 0.1219 and wR_2 = 0.3541. R indices (all data): R_1 = 0.1530 and wR_2 = 0.3741. Largest residual electron densities: 0.560 and –0.641 e Å^{-3}.

Table S27. Cartesian coordinates (in Å) for the crystal structure of **2** presenting static orientational disorder over six orientations.

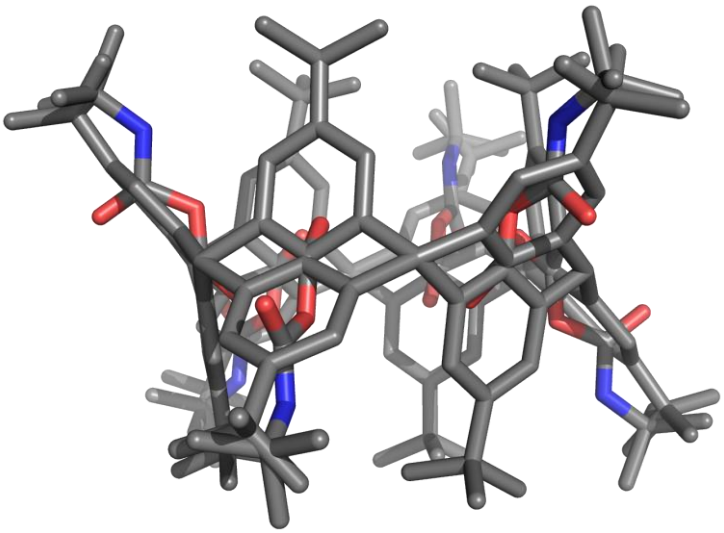

C	25.814000	0.792000	13.402000	C	27.616000	3.381000	15.718000
C	25.651000	-0.386000	12.666000	C	28.788000	3.603000	16.407000
C	25.886000	-0.386000	11.289000	C	29.831000	4.108000	15.674000
C	26.280000	0.740000	10.600000	C	29.779000	4.281000	14.286000
C	26.365000	1.896000	11.333000	C	28.992000	3.397000	17.911000
C	26.189000	1.937000	12.721000	C	30.045000	2.353000	18.184000
C	26.561000	0.814000	9.096000	C	27.669000	2.969000	18.536000
C	27.992000	1.204000	8.823000	C	29.437000	4.705000	18.523000
C	26.270000	-0.546000	8.471000	C	28.076000	5.340000	11.781000
C	25.651000	1.853000	8.484000	C	27.409000	6.362000	9.679000
C	24.421000	0.992000	15.226000	C	27.533000	5.890000	8.268000
C	23.202000	0.926000	17.328000	C	25.919000	6.555000	9.998000
C	23.673000	0.797000	18.739000	C	28.010000	7.743000	9.901000
C	22.290000	-0.269000	17.008000	N	27.980000	5.301000	10.474000
C	22.307000	2.136000	17.106000	O	28.544000	4.159000	12.255000
N	24.406000	0.890000	16.532000	O	27.740000	6.220000	12.516000
O	25.677000	0.806000	14.752000	C	28.589000	4.150000	13.400000
O	23.490000	1.141000	14.491000	C	27.294000	4.136000	12.885000
C	25.708000	0.841000	13.607000	C	26.929000	5.074000	11.910000
C	25.072000	-0.287000	14.121000	C	27.815000	5.962000	11.348000
C	24.078000	-0.135000	15.097000	C	29.116000	5.878000	11.794000
C	23.751000	1.077000	15.659000	C	29.517000	5.006000	12.809000
C	24.474000	2.162000	15.213000	C	27.566000	6.831000	10.113000
C	25.430000	2.072000	14.198000	C	26.636000	7.971000	10.425000
C	22.874000	1.295000	16.893000	C	28.913000	7.375000	9.634000
C	21.422000	1.060000	16.582000	C	26.964000	5.962000	9.036000
C	23.076000	2.734000	17.372000	O	29.038000	3.217000	14.284000
C	23.326000	0.340000	17.971000	C	26.228000	3.294000	13.566000
O	26.739000	0.763000	12.723000	C	27.228000	-3.241000	13.605000
C	25.268000	-1.632000	13.441000	C	28.167000	-3.971000	14.341000
C	28.600000	4.034000	13.605000	C	28.285000	-3.768000	15.718000
C	27.498000	3.585000	14.341000	C	27.506000	-2.864000	16.407000

C	26.548000	-2.212000	15.674000
C	26.424000	-2.344000	14.286000
C	27.582000	-2.583000	17.911000
C	27.960000	-1.149000	18.184000
C	28.615000	-3.515000	18.536000
C	26.228000	-2.852000	18.523000
C	26.358000	-4.348000	11.781000
C	25.806000	-5.436000	9.679000
C	26.153000	-5.093000	8.268000
C	26.384000	-6.824000	9.998000
C	24.310000	-5.607000	9.901000
N	26.439000	-4.412000	10.474000
O	27.147000	-3.353000	12.255000
O	25.764000	-5.080000	12.516000
C	27.133000	-3.309000	13.400000
C	27.792000	-4.423000	12.885000
C	27.162000	-5.208000	11.910000
C	25.950000	-4.885000	11.348000
C	25.372000	-3.716000	11.794000
C	25.927000	-2.934000	12.809000
C	25.322000	-5.536000	10.113000
C	24.800000	-6.911000	10.425000
C	24.177000	-4.641000	9.634000
C	26.376000	-5.622000	9.036000
O	27.716000	-2.454000	14.284000
C	29.054000	-4.926000	13.566000
C	31.428000	-4.034000	13.402000
C	32.529000	-3.585000	12.666000
C	32.412000	-3.381000	11.289000
C	31.240000	-3.603000	10.600000
C	30.196000	-4.108000	11.333000
C	30.249000	-4.281000	12.721000
C	31.035000	-3.397000	9.096000
C	29.982000	-2.353000	8.823000
C	32.359000	-2.969000	8.471000
C	30.591000	-4.705000	8.484000
C	31.951000	-5.340000	15.226000
C	32.618000	-6.362000	17.328000
C	32.494000	-5.890000	18.739000
C	34.109000	-6.555000	17.008000
C	32.018000	-7.743000	17.106000
N	32.047000	-5.301000	16.532000
O	31.484000	-4.159000	14.752000
O	32.288000	-6.220000	14.491000
C	31.439000	-4.150000	13.607000
C	32.734000	-4.136000	14.121000
C	33.099000	-5.074000	15.097000
C	32.213000	-5.962000	15.659000
C	30.911000	-5.878000	15.213000
C	30.511000	-5.006000	14.198000
C	32.462000	-6.831000	16.893000
C	33.392000	-7.971000	16.582000
C	31.115000	-7.375000	17.372000
C	33.064000	-5.962000	17.971000
O	30.990000	-3.217000	12.723000
C	33.800000	-3.294000	13.441000
C	32.800000	3.241000	13.402000
C	31.861000	3.971000	12.666000
C	31.743000	3.768000	11.289000
C	32.521000	2.864000	10.600000
C	33.480000	2.212000	11.333000
C	33.603000	2.344000	12.721000
C	32.445000	2.583000	9.096000
C	32.067000	1.149000	8.823000
C	31.412000	3.515000	8.471000
C	33.800000	2.852000	8.484000
C	33.669000	4.348000	15.226000
C	34.221000	5.436000	17.328000
C	33.874000	5.093000	18.739000
C	33.643000	6.824000	17.008000
C	35.717000	5.607000	17.106000
N	33.588000	4.412000	16.532000
O	32.880000	3.353000	14.752000
O	34.263000	5.080000	14.491000
C	32.895000	3.309000	13.607000
C	32.236000	4.423000	14.121000
C	32.865000	5.208000	15.097000
C	34.078000	4.885000	15.659000
C	34.656000	3.716000	15.213000
C	34.101000	2.934000	14.198000
C	34.706000	5.536000	16.893000
C	35.228000	6.911000	16.582000
C	35.851000	4.641000	17.372000
C	33.652000	5.622000	17.971000
O	32.312000	2.454000	12.723000
C	30.973000	4.926000	13.441000
C	34.214000	-0.792000	13.605000
C	34.376000	0.386000	14.341000
C	34.141000	0.386000	15.718000
C	33.747000	-0.740000	16.407000
C	33.662000	-1.896000	15.674000
C	33.839000	-1.937000	14.286000
C	33.467000	-0.814000	17.911000
C	32.036000	-1.204000	18.184000
C	33.758000	0.546000	18.536000
C	34.377000	-1.853000	18.523000
C	35.607000	-0.992000	11.781000
C	36.826000	-0.926000	9.679000
C	36.355000	-0.797000	8.268000
C	37.738000	0.269000	9.998000
C	37.721000	-2.136000	9.901000
N	35.621000	-0.890000	10.474000
O	34.350000	-0.806000	12.255000
O	36.538000	-1.141000	12.516000
C	34.320000	-0.841000	13.400000
C	34.956000	0.287000	12.885000
C	35.950000	0.135000	11.910000
C	36.276000	-1.077000	11.348000
C	35.553000	-2.162000	11.794000
C	34.598000	-2.072000	12.809000
C	37.154000	-1.295000	10.113000
C	38.606000	-1.060000	10.425000
C	36.951000	-2.734000	9.634000
C	36.702000	-0.340000	9.036000
O	33.288000	-0.763000	14.284000
C	34.759000	1.632000	13.566000

Table S28. Cartesian coordinates (in Å) for the single orientation of **2** deduced from the disordered crystal structure.

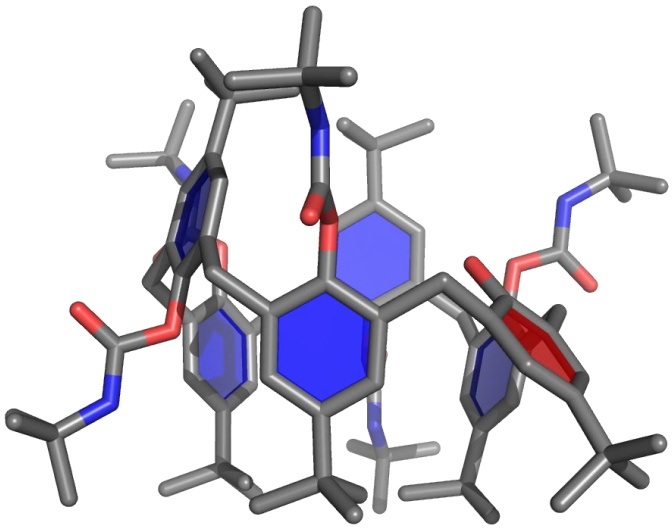

C	26.601000	4.035000	13.605000	C	30.036000	-1.203000	18.184000
C	25.226000	-3.241000	13.605000	C	19.416000	1.067000	16.582000
C	29.427000	-4.035000	13.402000	C	25.669000	2.970000	18.536000
C	30.801000	3.241000	13.402000	C	26.615000	-3.515000	18.536000
C	32.214000	-0.793000	13.605000	C	30.359000	-2.970000	8.471000
C	23.707000	0.842000	13.611000	C	29.413000	3.515000	8.471000
C	25.498000	3.586000	14.341000	C	31.758000	0.546000	18.536000
C	26.166000	-3.971000	14.341000	C	21.085000	2.734000	17.379000
C	30.529000	-3.586000	12.666000	C	27.437000	4.707000	18.523000
C	29.861000	3.971000	12.666000	C	24.226000	-2.853000	18.523000
C	32.377000	0.386000	14.341000	C	28.591000	-4.707000	8.484000
C	23.072000	-0.286000	14.125000	C	31.801000	2.853000	8.484000
C	25.616000	3.382000	15.718000	C	32.378000	-1.854000	18.523000
C	26.284000	-3.768000	15.718000	C	21.319000	0.340000	17.973000
C	30.412000	-3.382000	11.289000	O	26.543000	4.158000	12.254000
C	29.744000	3.768000	11.289000	O	25.148000	-3.353000	12.254000
C	32.142000	0.386000	15.718000	O	29.485000	-4.158000	14.752000
C	22.078000	-0.136000	15.097000	O	30.880000	3.353000	14.752000
C	26.788000	3.603000	16.407000	O	32.350000	-0.805000	12.254000
C	25.507000	-2.863000	16.407000	O	24.738000	0.764000	12.723000
C	29.239000	-3.603000	10.600000	C	26.077000	5.340000	11.780000
C	30.521000	2.863000	10.600000	C	24.358000	-4.348000	11.780000
C	31.747000	-0.740000	16.407000	C	29.951000	-5.340000	15.226000
C	21.750000	1.077000	15.664000	C	31.670000	4.348000	15.226000
C	27.830000	4.107000	15.675000	C	33.607000	-0.992000	11.780000
C	24.548000	-2.213000	15.675000	O	25.739000	6.220000	12.516000
C	28.197000	-4.107000	11.332000	O	23.764000	-5.080000	12.516000
C	31.479000	2.213000	11.332000	O	30.289000	-6.220000	14.490000
C	31.663000	-1.895000	15.675000	O	32.263000	5.080000	14.490000
C	22.474000	2.162000	15.218000	O	34.538000	-1.140000	12.516000
C	27.778000	4.280000	14.285000	N	25.981000	5.301000	10.475000
C	24.425000	-2.344000	14.285000	N	24.439000	-4.411000	10.475000
C	28.249000	-4.280000	12.722000	N	30.046000	-5.301000	16.532000
C	31.602000	2.344000	12.722000	N	31.588000	4.411000	16.532000
C	31.838000	-1.936000	14.285000	N	33.621000	-0.890000	10.475000
C	23.431000	2.072000	14.192000	C	25.410000	6.364000	9.679000
C	26.993000	3.399000	17.911000	C	23.805000	-5.437000	9.679000
C	25.581000	-2.584000	17.911000	C	30.618000	-6.364000	17.328000
C	29.035000	-3.399000	9.096000	C	32.223000	5.437000	17.328000
C	30.447000	2.584000	9.096000	C	34.827000	-0.927000	9.679000
C	31.468000	-0.815000	17.911000	C	25.533000	5.888000	8.268000
C	20.873000	1.296000	16.893000	C	24.155000	-5.092000	8.268000
C	28.045000	2.353000	18.184000	C	30.494000	-5.888000	18.739000
C	25.960000	-1.150000	18.184000	C	31.873000	5.092000	18.739000
C	27.983000	-2.353000	8.823000	C	34.353000	-0.796000	8.268000
C	30.067000	1.150000	8.823000	C	23.918000	6.555000	9.998000

C	24.385000	-6.825000	9.998000
C	32.109000	-6.555000	17.009000
C	31.643000	6.825000	17.009000
C	35.739000	0.269000	9.998000
C	26.009000	7.742000	9.901000
C	22.312000	-5.607000	9.901000
C	30.018000	-7.742000	17.106000
C	33.716000	5.607000	17.106000
C	35.720000	-2.135000	9.901000
C	23.270000	-1.633000	13.441000
C	24.228000	3.292000	13.566000
C	27.056000	-4.925000	13.566000
C	31.800000	-3.292000	13.441000
C	28.972000	4.925000	13.441000
C	32.758000	1.633000	13.566000

References

[1] Lavendomme, R.; Leroy, A.; Luhmer, M.; Jabin, I. *J. Org. Chem.* **2014**, *79*, 6563–6570.
[2] Rigaku Oxford Diffraction, 2017, CrysAlisPro Software system, version 38.46, Rigaku Corporation, Oxford, UK
[3] Sheldrick, G. M. Acta Cryst. **2015**, *A71*, 3–8.
[4] Sheldrick, G. M. Acta Cryst. **2015**, *C71*, 3–8.
[5] Dolomanov, O. V.; Bourhis, L. J.; Gildea, R. J.; Howard, J. A. K.; Puschmann, H. *J. Appl. Cryst.* **2009**, *42*, 339–341.
[6] Spek, A. L. *Acta Cryst.* **2015**, *C71*, 9–18.
[7] Allan, D.; Nowell, H.; Barnett, S.; Warren, M.; Wilcox, A.; Christensen, J.; Saunders, L.; Peach, A.; Hooper, M.; Zaja, L.; Patel, S.; Cahill, L.; Marshall, R.; Trimnell, S.; Foster, A.; Bates, T.; Lay, S.; Williams, M.; Hathaway, P.; Winter, G.; Gerstel, M.; Wooley, R. A. *Crystals* **2017**, *7*, 336.
[8] a) Collaborative Computational Project, Number 4. The CCP4 suite: programs for protein crystallography. *Acta Cryst.* **1994**, *D50*, 760–763. b) Evans, P. *Acta Cryst.* **2006**, *D62*, 72–82. c) Winter, G. *J. Appl. Crystallogr.* **2010**, *43*, 186–190.
[9] Farrugia, L. *J. Appl. Crystallogr.* **2012**, *45*, 849–854.
[10] Spek, A. L. *Acta Cryst.* **2009**, *D65*, 148–155.